BERITA SEDIMENTOLOGI

Number 45
05/2020

Indonesian Journal of Sedimentary Geology

ISSN 0853-9413



Published by
The Indonesian Sedimentologists Forum (FOSI)
The Sedimentology Commission - The Indonesian Association of Geologists (IAGI)

Editorial Board

Minarwan
Chief Editor
Bangkok, Thailand
E-mail: **minarwanx@gmail.com**

Herman Darman
Deputy Chief Editor
Petronas
Kuala Lumpur, Malaysia
E-mail: **herman_darman@yahoo.com**

Ricky Andrian Tampubolon
FOSI General Secretary
Odira Energy Karang Agung
E-mail: **rickyandriantampubolon@gmail.com**

Ragil Pratiwi
Layout editor
Patra Nusa Data, Jakarta
E-mail: **ragpratiwi@gmail.com**

Mellinda Arisandy
Social Media Coordinator & Head of FOSI Talk
Petronas, Jakarta, Indonesia
E-mail: **mellindaarisandy@yahoo.com**

Visitasi Femant
Treasurer, Membership & Social Media Coordinator
Pertamina Hulu Energi, Jakarta, Indonesia
E-mail: **fvisitasi@yahoo.com**

Maradona Mansyur
Beicip Franlab, Kuala Lumpur
E-mail: **maradona.mansyur042@yahoo.com**

Advisory Board



Prof. Yahdi Zaim
Quaternary Geology
Institute of Technology, Bandung

Prof. R. P. Koesoemadinata
Emeritus Professor
Institute of Technology, Bandung

Wartono Rahardjo
University of Gajah Mada, Yogyakarta, Indonesia

Mohammad Syaiful
Exploration Think Tank Indonesia

F. Hasan Sidi
Woodside, Perth, Australia

Prof. Dr. Harry Doust
Faculty of Earth and Life Sciences, Vrije Universiteit
De Boelelaan 1085
1081 HV Amsterdam, The Netherlands
E-mails: **harry.doust@falw.vu.nl**; **harrydoust@gmail.com**

Dr. J.T. (Han) van Gorsel
6516 Minola St., HOUSTON, TX 77007, USA
www.vangorselslist.com
E-mail: **jtvangorsel@gmail.com**

Dr. T.J.A. Reijers
Geo-Training & Travel
Gevelakkers 11, 9465TV Anderen, The Netherlands
E-mail: **tjareijers@hetnet.nl**

Dr. Andy Wight
formerly IIAPCO-Maxus-Repsol, latterly consultant for Mitra Energy Ltd, KL
E-mail: **yah1wight@yahoo.co.uk**



Cover Photograph:

Disharmonic folds in bedded chert, Noni Formation. Photo taken at the bank of Noil Noni River, West Timor (see p. 8)

Photo credit: Munasri & A.H. Harsolumakso

Berita Sedimentologi

- Published 3 times a year by the **Indonesian Sedimentologists Forum** (Forum Sedimentologiwan Indonesia, **FOSI**), a commission of the **Indonesian Association of Geologists** (Ikatan Ahli Geologi Indonesia, **IAGI**).
- Cover topics related to sedimentary geology, including their depositional processes, fossils, deformation, minerals, basin fill, etc.

Berita Sedimentologi

A sedimentological Journal of the Indonesia Sedimentologists Forum (FOSI), a commission of the Indonesian Association of Geologist (IAGI)



From the Editor

We are nearly at the middle of year 2020 and so far, many things look and feel completely different from how they did in the same period of recent years that have passed by. Right now, the world is still trying to control COVID-19 pandemic that have disrupted our lives and changed the way we do things globally. As of late May, there have been approx. 5.92 million cases recorded globally and the end of the pandemic is still unclear despite the slower growth of official cases in some countries. Drastic measures were applied by the government, borders were closed and all of the sudden we were urged to stay at home for several months. Airplanes were grounded and the streets were empty. The pandemic definitely will impact the world's economy because many businesses lost revenues and employees also lost their jobs.

The sudden drop in oil demand caused by the pandemic and production oversupply eventually drove Brent Crude price to below US$20/bbl (21st April 2020). This was a price level that had not been seen before for at least 18 years. While oil price has recovered to US$37-US$38/bbl right now, it is natural to expect that the industry will experience some "adjustments" in the near future to keep its operating cost low and postpone low profitability projects. Hopefully we all can sail through this challenging period smoothly as some of us have possibly done before in the past.

Despite the currently challenging situation, we are still able to deliver Berita Sedimentologi No. 45 to your desk and obviously we're also very grateful to receive manuscript submission and cooperation from the authors. Their contribution to Berita Sedimentologi is truly appreciated by the editorial board.

Our plan next is to publish Berita Sedimentologi No. 46 in August this year, so we're now inviting potential contributors to send us any manuscripts related to sedimentary geology, carbonate geology, basin analysis and petroleum geosciences. Please do contact us by email to discuss about your submission plan or to speak about anything related to Berita Sedimentologi. We're always happy to hear from you and in the meantime, we hope you find this volume useful. Happy reading!

Minarwan
Chief Editor

Contents

Late Cretaceous radiolarians from the Noni Formation, West Timor, Indonesia..... 5
Munasri and Agus H. Harsolumakso

A new insight of Talang Akar Formation in the Ridho Field, North Palembang Sub-basin, Indonesia: An integrated approach..... 19
Togi Y. Sitinjak, Ricky A. Tampubolon, Ardian Pratama, Wildanto P. Nusantara, Aziza Muis and Harsanti Setiani

Sedimentary basins of Indonesia: Outline and thickness variation understanding..... 39
Herman Darman and Doddy Yuliong B.A.

About FOSI

The forum was founded in 1995 as the Indonesian Sedimentologists Forum (FOSI). This organization is a communication and discussion forum for geologists, especially for those dealing with sedimentology and sedimentary geology in Indonesia.

The forum was accepted as the sedimentological commission of the Indonesian Association of Geologists (IAGI) in 1996. About 300 members were registered in 1999, including industrial and academic fellows, as well as students.

FOSI has close international relations with the Society of Sedimentary Geology (SEPM) and the International Association of Sedimentologists (IAS).
Fellowship is open to those holding a recognized degree in geology or a cognate subject and non-graduates who have at least two years relevant experience.

FOSI has organized three international conferences in 1999, 2001 and the most recently in 2018.

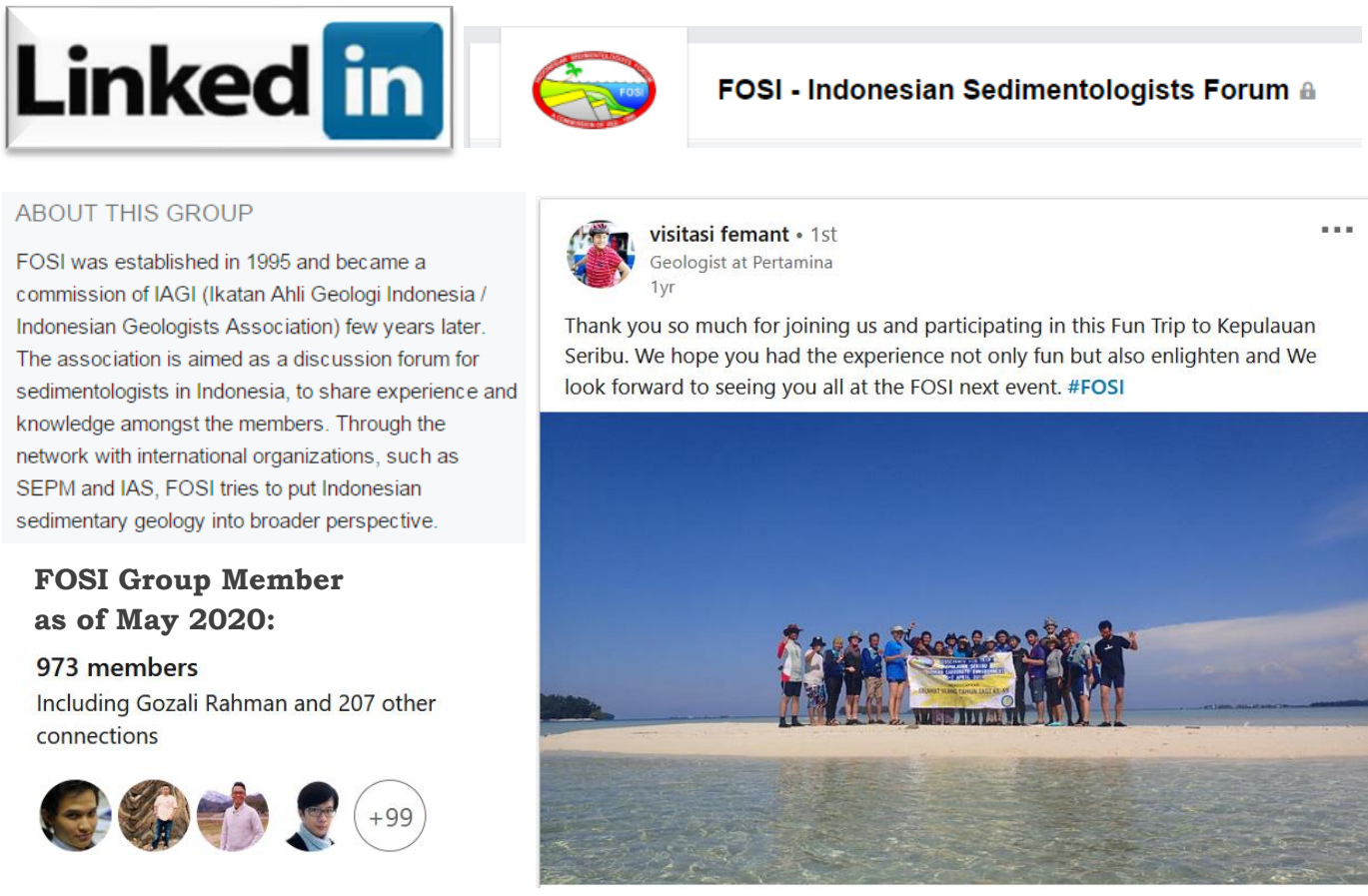
Most of FOSI administrative work will be handled by the editorial team. IAGI office in Jakarta will help if necessary.

The official website of FOSI is:

http://www.iagi.or.id/fosi/

FOSI Membership

Any person who has a background in geoscience and/or is engaged in the practising or teaching of geoscience or its related business may apply for general membership. As the organization has just been restarted, we use **LinkedIn** (**www.linkedin.com**) as the main data base platform. We realize that it is not the ideal solution, and we may look for other alternative in the near future. Having said that, for the current situation, LinkedIn is fit for purpose. International members and students are welcome to join the organization.



LATE CRETACEOUS RADIOLARIANS FROM THE NONI FORMATION, WEST TIMOR, INDONESIA

Munasri [1,#] and Agus Handoyo Harsolumakso [2]

[1]Formerly Pusat Penelitian Geoteknologi LIPI; Sekolah Tinggi Teknologi Mineral Indonesia, Bandung.
[2]Faculty of Earth Sciences and Technology, Institut Teknologi Bandung, Bandung (deceased on October 18th, 2019).
[#]Corresponding author at irsanum@yahoo.co.id

ABSTRACT

Late Cretaceous (Cenomanian–Turonian) radiolarian fauna was recovered from a single chert sample of the Noni Formation in the Miomaffo District of West Timor, which is generally viewed as part of the allochthonous 'Banda Terrane'. This fauna is characterized by the presence of Cryptamphorella conara, Diacantocapsa euganea, Dictyomitra formosa, Dictyomitra montisserei, Guttacapsa biacuta, Stichomitra communis, Patelula verteroensis, Pessagnobrachia fabianii, Praeconocaryomma lipmanae and others. The character of the radiolarian fauna shows a close resemblance to those in South Sulawesi and is very different from age-equivalent radiolarian faunas in the 'autochthonous' southern foldbelts of West Timor (Kolbano) and Timor Leste (Viqueque). This report on the Late Cretaceous radiolarians in Timor attempts to identify the fauna, to clarify its age, and to indicate the paleogeographic origin of radiolarian-bearing chert of the Noni Formation.

Keywords: Noni Formation, Late Cretaceous radiolarians, West Timor, Timor Leste

INTRODUCTION

Since Tan (1927) described the radiolarian assemblage in Rotti Island, occurrences of radiolarians in West Timor and Rotti Island have largely been considered in any detail only by the present authors since the 1990s. We have discussed radiolarian assemblages within the age ranges Triassic–Late Jurassic (Harsolumakso et al., 1995; Kolbano area), Middle Triassic (Sashida et al., 1999; Kefamenanu area), Late Triassic (Sashida et al., 1996; Nefokoko area; Martini et al., 2000; Niki-Niki, Soe and Kapan areas), Middle Jurassic (Sashida et al., 1999; Rotti Island) and Early Cretaceous (Munasri and Sashida, 2018, Clove, 1997, Munasri, 1998; Kolbano area). In the eastern part of Timor Island (Timor Leste), Middle Jurassic radiolarians were reported by Keep et al. (2009) and discussed by Haig and Bandini (2013).

The present paper concerns Late Cretaceous radiolarians from chert of the Noni Formation, in West Timor (Figure 1). The radiolarian-bearing cherts of the Noni Formation were considered to be of Late Jurassic or Early Cretaceous age (Haile et al., 1979; Earle, 1983). Previously, Audley Charles et al. (1974) suggested a possible Aptian age for the Palelo (Noni Formation) green cherts, unconformably overlain by Turonian (?) cherty limestones and black cherts. Haile et al. (1979) compared the Noni Formation chert sequences to those in the Bantimala area of South Sulawesi, which were then only dated as broadly Jurassic–Cretaceous in age. Now we know the cherts sequence exposed in the Paring River, Bantimala area of South Sulawesi, is of Albian to Cenomanian (middle Cretaceous) age (Wakita et al., 1994). Haig and Bandini (2013) referred to the Noni Formation as a correlative of a Middle Jurassic black argillite block in mélange sampled near Viqueque, Timor Leste, based on the radiolarian assemblage comparisons that they made with the Middle Jurassic succession in the Kolbano area of West Timor (Harsolumakso et al., 1995). Disputes on the age and origin of the Noni Formation will be discussed further later.

The primary aims of this paper are: (1) to identify the radiolarian fauna, (2) to clarify its age, and (3) to consider the possible paleogeographic origin of the radiolarian chert in the Noni Formation.

AHH (the second author) conducted a field survey and obtained rock samples along the Noil Noni River, in the Miomaffo region of West Timor. The first author (M) then washed one chert sample, NN02AH, to examine the radiolarian content.

GEOLOGICAL SETTING

The Noni Formation, named after the Noil Noni River was described by Rosidi et al. (1979) as a unit of

deep-sea sedimentary rocks comprising well-bedded mainly greenish radiolarian chert, with cherty limestone and clayey chert. The cherts of the Noni Formation, typically bedded on a scale of 5–15 cm thickness, is highly deformed and folded with irregular fold axis and broken bedding planes.

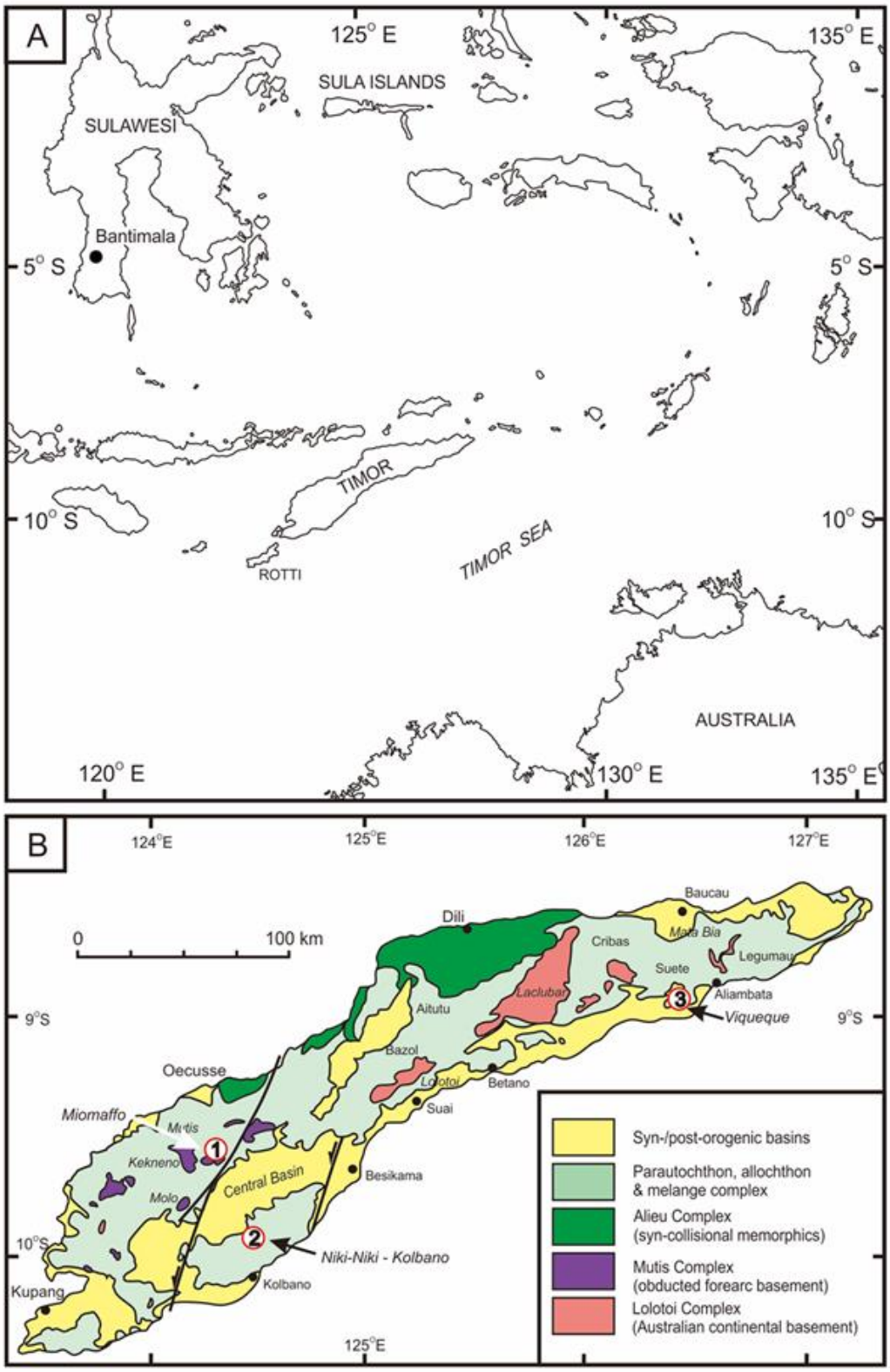


Figure 1: *Maps of Eastern Indonesia and Timor Island, showing the location of studies related to radiolaria. (A) Location and names of islands where radiolaria are found as mentioned and compared in this paper: Timor Island (see Figure 1B), Bantimala area, South Sulawesi studied by Wakita et al. (1994), and Sula Islands described by Pessagno and Hull (2002). (B) Locations of radiolarians findings on Timor Island discussed in this paper: (1) Late Cretaceous radiolarians of the Noni Formation in the Miomaffo region. (2) Middle to Late Jurassic radiolarians in the Kolbano to Niki-niki area (Harsolumakso et al., 1995) and (3) Middle Jurassic radiolarians near Viqueque, East Timor (Haig and Bandini, 2013).*

Rosidi et al. (1979) proposed the Noni and Haulasi Formations as units together forming the Palelo Group (Palelo Series of Tappenbeck 1940, Van West 1941). The Palelo Group is a Cretaceous to Eocene sedimentary and volcanic succession that overlies the Mutis metamorphic rocks, and comprises a lower deep-water unit and an upper shallow water unit. The lower Palelo Group corresponds to the Noni Formation. Fossil *Globotruncana* sp. found in the cherty limestone indicates a Late Cretaceous age (Rosidi et al., 1979). The upper Palelo Group, corresponding to the Haulasi Formation, consists of conglomeratic graywacke, sandstone, tuffaceous shale, bedded marl, and limestone. Middle Paleocene to Middle Eocene foraminifera (*Nummulites* sp., *Alveolina* sp.) were found in limestones (Rosidi et al., 1979). Preliminary age determinations for the presumed Haulasi Formation in the Samé area of Timor Leste were reported by Charlton et al. (2018). Six genera and one species of dinoflagellates were recorded (*Exochosphaeridium* sp., *Florentinia* sp., *Heterosphaeridium* sp., *Odontochitina* sp., *Palaeohystrichophora infusorioides*, *Spiniferites* sp. and *Subtilisphaera* sp.), all of which have been identified in numerous petroleum exploration wells drilled on the Australian continental margin to the south of Timor. For instance, all seven genera/species occur in the late Albian-early Cenomanian interval in the Mount Ashmore-1B well.

Harris (2006) reported that an andesitic clast in a conglomerate of the typical Haulasi Formation found in the Bebe Susu massif, Timor Leste yielded a U/Pb age of 83 Ma (approximately Santonian-Campanian). The Palelo Group in West Timor is overlain by Eocene deposits of the Metan Formation (Rosidi et al., 1979), which consists of agglomerates with tuffaceous matrix and components of pumice, pyroxene basalt and andesite lava, and andesitic and dacitic tuffs, and represent a part of the Eocene 'Great Indonesian Arc' of Haris (2006). The upper part contains lenses of limestone and sandy marl with Early Eocene foraminifera. A dacitic tuff from the Mosu massif in West Timor yielded an U/Pb age of 35 Ma (approximately Late Eocene) (Harris, 2006).

In terms of tectonostratigraphy, rock assemblages in Timor are frequently described in term of allochthonous, autochthonous and para-autochthonous elements (for details see previous authors e.g. Audley Charles, 1968; Carter et al., 1976, Barber et al., 1977, Charlton et al., 1991; Harsolumakso et al., 1995). The Palelo Group (including the Noni Formation) and the underlying Mutis metamorphic complex (Haile et al., 1979; Earle, 1983) were described as elements of the Banda Terrane (Sopaheluwakan, 1990; Harris, 2006) which is interpreted as an allochthonous body overthrust onto the para-autochthonous Australian margin successions of Timor Island.

MATERIAL AND METHODS

One sample of chert, NN02AH originating from the bedded chert layer of the Noni Formation, was collected from the succession exposed in the Noil Noni River near Noil Toko Village, Subdistrict of Miomaffo Barat in the District of Timor Tengah Utara, West Timor (Figure 2 and Figure 3). The chert sample was crushed into 1-2 cm fragments and soaked in dilute 1 % to 5 % hydrofluoric acid (HF) for about 24 hours (Pessagno & Newport, 1972). The acid then was discarded and the sample washed, sieved and dried. Radiolarians within the sample residue were picked under a binocular microscope. Most of the obtained radiolarians have poor to very poor preservation. Radiolarian images presented were photographed using a Scanning Electron Microscope (SEM) in the Geological Department of the Institut Teknologi Bandung, Indonesia. Identified radiolarians are listed in Table 1 and are illustrated in Plates 1 and 2.

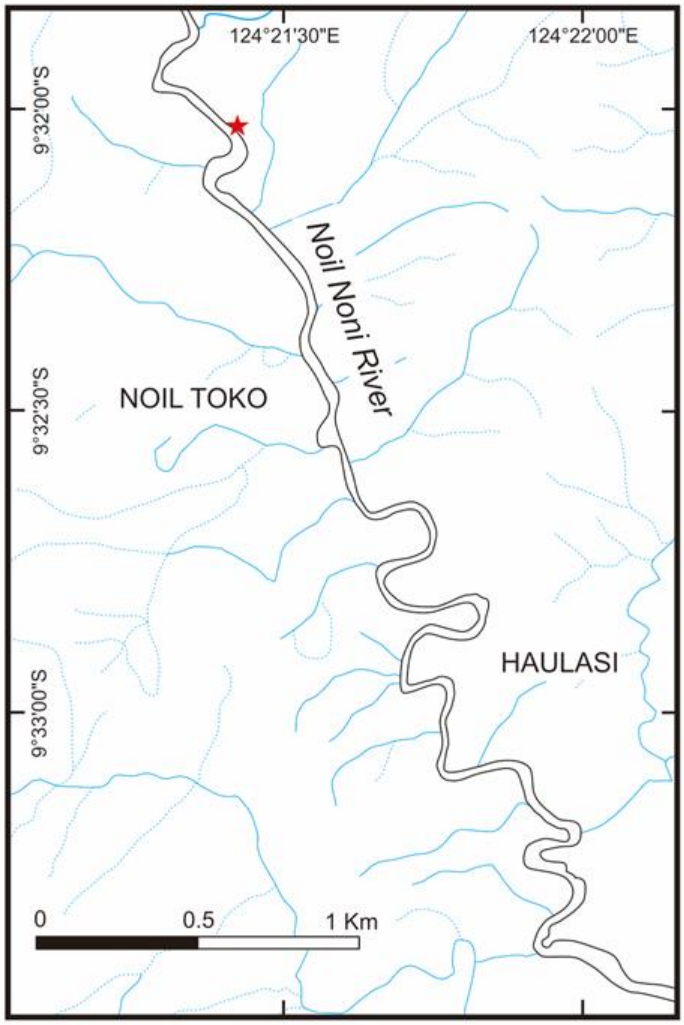


Figure 2: *Map showing sample location (red star) for radiolarian-bearing chert in the Noil Noni River in the Miomaffo region, West Timor.*



Figure 3: *Disharmonic folds in bedded chert of the Noni Formation in the bank of Noil Noni River, West Timor as shown in Figure 2.*

RADIOLARIAN FAUNA AND AGE

A total of 35 specimens comprising 15 genera and 1 indeterminable species are presented in this paper. Among them, 11 species are used for age determination: *Cryptamphorella conara* (Foreman), *Diacanthocapsa euganea* Squinabol, *Dictyomitraformosa* Squinabol, *Dictyomitra montisserei* (Squinabol), *Guttacapsa biacuta* (Squinabol), *Squinabollum fossilis* (Squinabol), *Stichomitra communis* Squinabol, *Paronaella communis* (Squinabol), *Pessagnobrachia fabianii* (Squinabol), *Pessagnobrachia irregularis* (Squinabol), and *Praeconocaryomma lipmanae* Pessagno.

From the full faunal list, 11 species were originally described from Italy (Mediterranean region) (Squinabol, 1903, 1904, 1914; O'Dogherty, 1994), and 8 of which can be used for age determination. We use the basic range-chart of O'Dogherty (1994) based on the Unitary Association Zones (U. A. Zones) (Figure 4). As there is no standard radiolarian biochronology available for the Late Cretaceous (Bandini et al., 2006), we sought to compare several other published radiolarian zonation schemes. For this study the biostratigraphic range of certain radiolarian species based on the Unitary Association is compared with those established in the following selected 7 publications: Bak (2011; Italy and Poland), Dumitrica (1970; Romania), Pessagno (1976; California), Sanfilippo & Riedel (1985; composite), Taketani (1982; Japan), Thurow (1988; Atlantic), and Tumanda (1989; Japan, composite) [Figure 4]. Based on the presence of the above mentioned species, a most likely Cenomanian–Turonian (early Late Cretaceous) age can be assigned for the radiolarian assemblage of the Noni Formation. It is possible that the age is slightly older (Cenomanian until the late Albian), but it will not be younger than Turonian as the last occurrences of *Cryptamphorella conara, Diacantocapsa euganea, Stichomitra communis* and *Praeconocaryomma lipmanae* are up to the end of the Turonian (Dumitrica, 1970, Taketani, 1982, Thurow, 1988). Using only the Unitary Association zonation of Dogherty (1994), the age range of the Noni Formation sample is within U.A. Zone 17 (middle Cenomanian). It is possibly one fairly precise age determination within a formation that has an as-yet undetermined broader age range.

Comparing with radiolarian faunas from northern Hokkaido, Japan (Tumanda, 1989), the similar presence of *Stichomitra communis*, *Squinabollum fossilis*, *Dictyomitra densicostata* (here identified as *D. montesserei*), *Stichomitra cf. stocki*, suggests the radiolarian assemblage from the Noni Formation is correlative with her *Thanarla praevenata–Holocriptocanium geyserenses* to *Alieveum praegallowayi–Amphipyndax* sp. A Assemblage Zones within the Cenomanian to Turonian–Coniacian age range. In Italy 12 species described by Bak (2011), including *Cryptamphorela conara,*

Diacanthocapsa euganea, Dictomitra formosa, Dictyomitra montesserei, Guttacapsa biacuta, Squinabollum fossilis, Stichomitra communis, Paronaella communis, Patellula verteroensis, Pessagnobrachia fabianii, Pessagnobrachia irregularis, and *Praeconcaryomma lipmanae*, of upper Cenomanian–lower Turonian age, are also present in the radiolarian assemblage of the Noni Formation. Using the above studies, we interpret the best fit age for the Noni Formation sample is within the Cenomanian–Turonian (100.5–89.8 Ma; International Commission on Stratigraphy, 2019).

DISCUSSION

The occurrence of well-known species such as *Dictyomitra formosa, Diacanthocapsa euganea, Stichomitra communis, Cryptamphorella conara,* together with *Guttacapsa biacuta* and *Praeconoaryomma lipmanea* undoubtedly determine the Noni Formation as having an early Late Cretaceous age (Cenomanian–Turonian). However, it is not clear yet if this age is representative of the entire chert of the Noni Formation, or whether this chert sequence may have a broader age range.

Haig and Bandini (2013) considered that Middle Jurassic black shales and green to white radiolarian cherts in Harsolumakso et al.'s (1995) Succession E, exposed in the Kolbano region of West Timor are equivalent to the Noni Formation (Palelo Group). However, Harsolumakso et al. (1995) did not interpret their Succession E (dated as Aalenian–Tithonian) as stratigraphic equivalent of the Noni Formation. Haig and Bandini (2013) furthermore indicated that Succession E of Harsolumakso et al. (1995) has lithological similarity to thin bedded siliceous argillites in large blocks within a mélange unit near Viqueque in Timor Leste. Haig and Bandini (2013) interpreted their Viqueque successions as lithostratigraphically equivalent to Succession E in the Kolbano area (quoted by them as Noni Group). By establishing the Late Cretaceous age for radiolarian cherts of the Noni Formation, equating the Noni Formation with the Succession E of the Kolbano area and correlating it to that in the siliceous argillites mélange block near Viqueque, Timor Leste is no longer appropriate. The siliceous argillite blocks in mélange near Viqueque in Timor Leste may correspond with the black shale of Succession E in the Kolbano area of West Timor (Harsolumakso et al., 1995), but we consider that the Jurassic successions in both Timor Leste (Haig and Bandini, 2013) and Succession E (Harsolumakso et al., 1995) are better assigned to the Wai Luli Formation of Audley-Charles (1968).

The radiolarian fauna collected from the Noni Formation resembles that of the cherts in the Paring River in the Bantimala area of South Sulawesi, interpreted as late Albian–early Cenomanian age by Wakita et al. (1994b: previously examined by Haile et al., 1979). These two assemblages have several distinct taxa in common, such as *Cryptamphorella conara, Diacantocapsa euganea, Dictyomitra montisserei* (*Dictyomitra* sp. in Wakita et al., 1994) and *Stichomitra communis*. It seems that deposition of the Noni Formation radiolarian cherts occurred at the same time or soon after deposition of the cherts in Bantimala, South Sulawesi.

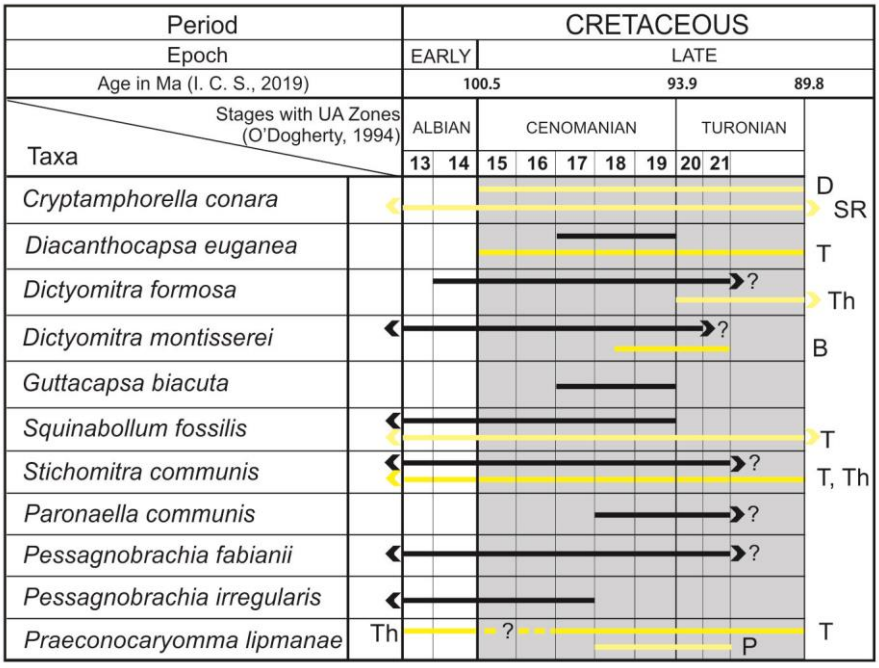


Figure 4: *Biostratigraphic range of selected radiolarian species compiled from various authors. Range-chart is adopted from O'Dogherty's (1994) Unitary Association Zones. The age-range indicated by black bars are from O'Dogherty (1994). In yellow are ranges suggested by D: Dumitrica (1970), SR: Sanfilippo and Riedel (1985), T: Taketani (1982), Th: Thurow (1980), B: Bak (2011), P: Pessagno (1976).*

Table 1: List of Late Cretaceous radiolarians from chert sample NN02AH of the Noni Formation, West Timor.

Plate 1	**Radiolarian species**
1.1.	*Dictyomitra formosa* Squinabol
1.2.	*Archaeodictyomitra* sp.
1.3.	*Stichomitra communis* Squinabol
1.4.	*Stichomitra communis* Squinabol
1.5.	*Stichomitra communis* Squinabol
1.6.	*Archaeodictyomitra* sp.
1.7.	*Dictymitra montisserei* (Squinabol)
1.8.	*Dictyomitra montisserei* (Squinabol)
1.9.	*Stichomitra stocki* (Campbell & Clark)
1.10.	*Novixitus* sp. cf. *N. mclaughlini* Pessagno
1.11.	*Dictyomitra montisserei* (Squinabol)
1.12.	*Dictyomitra montisserei* (Squinabol)
1.13.	*Pseudodictyomitra* sp. A.
1.14.	*Diacanthocapsa euganea* Squinabol
1.15.	*Guttacapsa biacuta* (Squinabol)
1.16.	*Dorypyle elliptica* Squinabol
1.17.	*Cryptamphorella conara* (Foreman)
1.18.	*Cryptamphorella* sp.
1.19.	*Squinabollum fossilis* (Squinabol)
Plate 2	Radiolarian species
2.1.	*Paronaella communis* (Squinabol)
2.2.	*Paronaella communis* (Squinabol)
2.3.	*Pessagnobrachia fabianii* (Squinabol)
2.4.	*Pessagnobrachia irregularis* (Squinabol)
2.5.	Spumellarian gen. et sp. indet.
2.6.	*Crucella* sp.
2.7.	*Crucella* sp.
2.8.	*Savaryella* sp.
2.9.	*Triactoma* sp. cf. *T. cellulosa* Foreman
2.10.	*Triactoma* sp. cf. *T. cellulosa* Foreman
2.11.	*Pseudoacanthosphaera* sp. cf. *P. spinosissima* (Squinabol)
2.12.	*Pseudoacanthosphaera* sp. cf. *P. spinosissima* (Squinabol)
2.13.	*Pessagnobrachia* sp.
2.14.	*Patelulla verteroensis* (Pessagno)
2.15.	*Praeconocaryomma lipmanae* Pessagno
2.16.	*Praeconocaryomma* sp. cf. *P. universa* Pessagno

Munasri and Sashida (2018) reported Early Cretaceous radiolaria from the Nakfunu Formation in the Kolbano area, West Timor. The composition of this fauna is quite different from that found in the Noni Formation (this report) and in the Bantimala area of South Sulawesi (Wakita et al., 1994). Approximately 35% of radiolarian taxa from the Nakfunu Formation have never been reported from the low-paleolatitude belt. Such taxa are attributed as "non-Tethyan fauna" by Baumgartner (1992, 1993). Conversely, radiolarian fauna from the Noni Formation and the Bantimala area of South Sulawesi share similarities with Alpine–Mediterranean, Central Atlantic, Central Pacific and Japanese samples, and are assigned to a "Tethyan fauna." This suggests the Noni Formation possibly formed at a lower paleolatitude or in a different paleo-oceanic current system from the Nakfunu Formation of the Kolbano area (Munasri and Sashida, 2018).

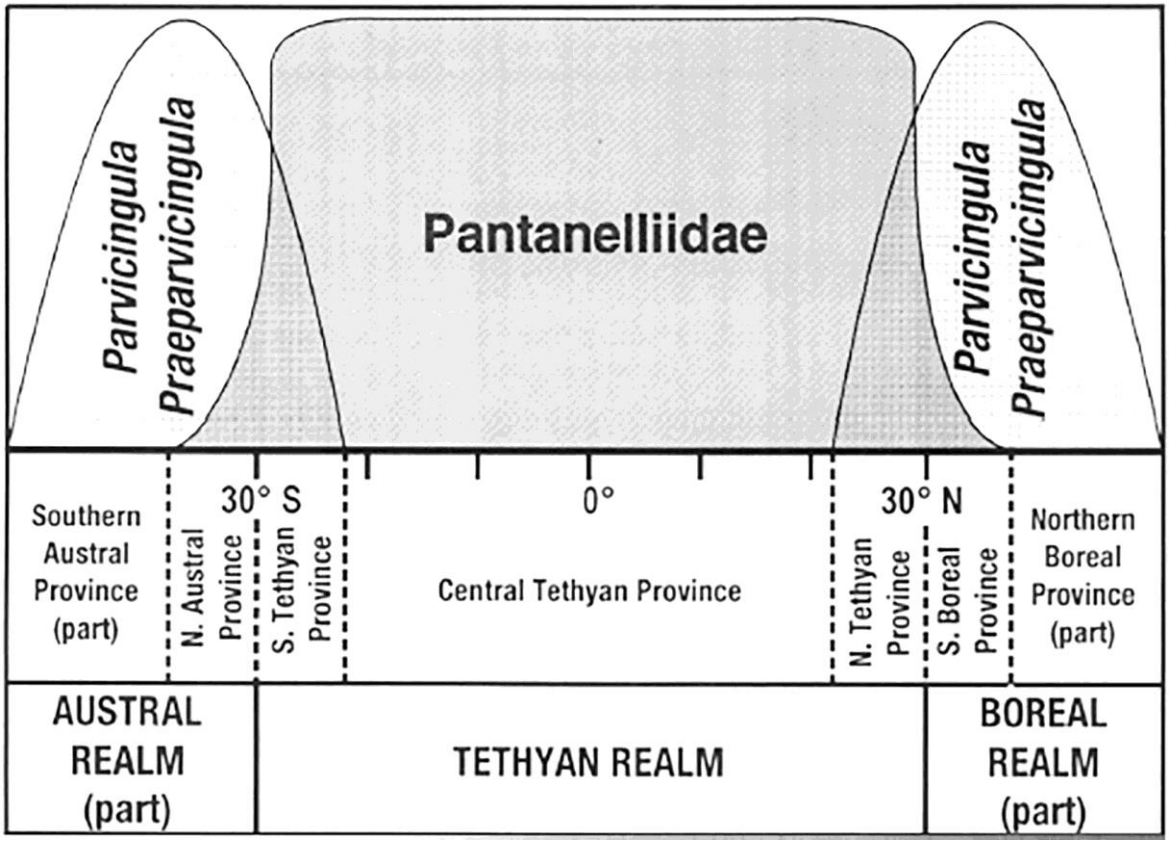


Figure 5: *Paleolatitudinal model based on distribution of selected Radiolaria from Jurassic and Lower Cretaceous (adopted from Pessagno and Hull, 2002).*

A classification of the paleolatitude zonation of radiolarians, especially for Jurassic faunas, was presented by e.g. Pessagno and Blome (1986), Pessagno and Hull (2002) and Hull (1995). Their paleolatitudinal model describes radiolarian distributions in the Tethyan and Boreal Realms (Figure 5). They suggested that some faunal elements described from Buya Formation assemblages in the Sula Islands are characteristic of the Northern Austral Province (Southern Hemisphere).

Regarding species described from a siliceous argillite block near Viqueque, East Timor (Haig and Bandini, 2013), which contain a common *Parvicingula / Praeparvicingula* fauna (one element of which is *Praeparvicingula hurdygurdyensis*), suggests a similarity with that obtained from the Buya Formation in the Sula Islands. In addition, some species in Haig and Bandini (2013)'s assemblage were identical to taxa found by Tan (1927) on Rotti Island, such as *Pseudodictyomitrella (= Stichocapsa)* singularis Tan and *Pseudodictyomitrella (=Cyrtocapsa) pseoudacerra* Tan. These taxa are not commonly found in the low paleolatitude belt, nor in a Tethyan faunas. We consider that the radiolarian faunas from the siliceous argillite near Viqueque in Timor Leste (Haig and Bandini, 2013) and possibly that from Succession E in the Kolbano area in West Timor (Harsolumakso et al., 1995) derived from the Northern Austral Province (Southern Hemisphere) as defined by Pessagno and Hull (2002). The Middle Jurassic Circum-Antarctic current conveyed the "non-Tethyan fauna" to the deposition place for the corresponding Wai Luli Formation in the northern Australian shelf and the paleogeographically related para-autochthonous successions of Timor. We consider that the Middle Jurassic radiolarian assemblages mentioned above faced similar occurrences with that fauna obtained from the Nakfunu Formation in West Timor during Early Cretaceous time (Munasri and Sashida, 2018).

Conversely, the Late Cretaceous radiolarian-bearing cherts from the Noni Formation (Palelo Group) were deposited in the low paleolatitude Tethyan realm as part of the Banda Terrane (Harris, 2006) and over-thrusted as an allochthonous element on Timor (Marks 1961, Carter et al. 1976, Earle 1983).

TAXONOMIC LIST AND REMARKS

The following radiolarian taxa are listed in alphabetical order under Suborders Nassellaria and Spumellaria. Remarks are given where needed, especially to explain the position of taxa, synonym explanation, and description of taxon that has not been previously recognized (e.g. *Pseudodictyomitra* sp. A.).

1. Suborder Nassellaria

Archaeodictyomitra spp.

Plate 1, Figures 2, 6.

Cryptamphorella sp.
Plate 1, Figure 18
Remarks: This form is included in the genus *Crypthamporella* by its general outline. Test spherical without aperture, showing the opposite side of cephalo-thorax or distal part of inflated abdomen.

Cryptamphorella conara (Foreman, 1968)
Plate 1, Figure 17
Hemicryptocapsa conara Foreman, 1968, p. 35, pl. 4, figs. 11a and 11b
Cryptamphorella conara (Foreman), Dumitrica, 1970, p. 80, pl. 11, figs. 66a–c; Taketani, 1982, p. 67, pl. 7, figs. 6a,b, 7a,b; Sanfilippo and Riedel, 1985, p. 613, text fig. 12.1a–c; Thurow, 1988, p. 399, pl. 1, fig. 2, and pl. 5, fig. 1; Bak, 2011, p. 87, figs. 43B,C.
Remarks: This species is common in the Cenomanian and Turonian (Dumitrica, 1970), spanning from Albian through Maastrichtian (Sanfilippo and Riedel, 1985).

Diacanthocapsa euganea Squinabol, 1903
Plate 1, Figure 14
Diacanthocapsa euganea Squinabol, 1903, p. 133, pI. 8, fig. 26; Taketani, 1982, p. 68, pl. 8, figs. 2a-3b; pl. 12, fig. 15; Tumanda, 1989, p. 36, pl. 7, fig. 5; O'Dogherty, 1994, p. 218, pl. 36. Figs. 19-21; Bak, 2011, p. 94, figs. 45I, J.
Remarks: Three-segmented cryptocephalic nasselarians. Due to poor preservation, our specimen shows an obscure apical horn. This species appears in the middle Cenomanian time (his U.A. Z. 17–19) of the Mediterranean region (O'Dogherty, 1994), Cenomanian – Turonian in Japan (Taketani, 1982).

Dictyomitra formosa Squinabol
Plate 1, Figure 1
Dictyomitra formosa Squinabol, 1904, p. 232, pl. X, fig. 4; Pessagno, 1976, p.51, pl. 8, figs. 10-12; Taketani, 1982, p. 58, pl. 4, figs. 6a,b and pl. 11, fig. 13; Thurow, 1988, p. 400, pl 1, fig. 25; Wakita, *et al.*, 1994a, figs. 5.1–3; figs. 6.1–3; O'Dogherty, 1994, p. 80, pl. 4, figs. 8–12; Bak, 2011, p. 98, figs. 47K–M; Asis & Basir Jasin, 2012, p. 90. Pl. 1, fig. 4.
Dictyomitra sp. cf. *D. formosa* Squinabol, Thurow, 1988, p. 400, pl 1, fig. 23.
Remarks: *D. formosa* Squinabol differs from *D. multicostata* Zittel *sensu stricto* by having deep strictures between the postabdominal chambers, more massive costae, a more markedly lobate test, and only weakly developed costae on the cephalis and thorax.

Dictyomitra montisserei (Squinabol, 1903)
Plate 1, Figures 7–8, 11–12
Stichophormis Montis Serei Squinabol, 1903, p. 137, pl. 8, fig. 38.
Archaeodictyomitra sliteri Pessagno, 1977, p. 43, pl. 6, figs. 3,4, 22, 23, 27; Tumanda, 1989, p. 36, pl. 7, fig. 2.
Dictyomitra sp. A. Taketani, 1982, p. 59, pl. 4, figs. 7a-b.
Dictyomitra densicostata Pessagno, Tumanda, 1989, p. 36, pl. 9, fig. 5.
Dictyomitra montisserei (Squinabol), O'Dogherty, 1994, p. 77, pl. 3, figs. 1–29; Bak, 2011, p. 100, figs. 48A–C.
Remarks: Form of slender, conical to cylindrical multi-segmented nasselarians, with costae throughout. Constrictions weak to well developed. The degree of preservation is very influential in distinguishing *Dictyomitra montisserei*, *Dictyomitra densicostata* and *Archaeodictyomitra sliteri*.

Dorypyle elliptica Squinabol, 1903b
Plate 1, Figure 16
Lithapium ellipticum Squinabol, p. 117, pl. 10, fig. 27.
Dorypyle elliptica Squinabol, O'Dogherty, 1994, p. 206, pl. 33, figs. 8–15.

Guttacapsa biacuta (Squinabol)
Plate 1, Figure 15
Cenellipsis biacutus Squinabol, p. 116, pl. 8, fig. 24.
Guttacapsa biacuta (Squinabol), O'Dogherty, p. 226, pl. 37, figs 31–35; Bak, 2011, p. 101, fig. 49A.

Pseudodictyomitra sp. A.
Plate 1, Figure 13
Remarks: The only one specimen of multi-segmented *Pseudodictyomitra* with seven post-abdominal chambers. Test elongate, slender, conical. Cephalis smooth, sharply pointed apically. Abdomen faintly costate. Single rings of primary pores are situated in strictures at joints separating adjacent segments; the first one separating thorax and abdomen. The post-abdominal chambers slowly increasing in width distally. Post-abdominal chambers with six to seven elongated thin and weakly costae visible in lateral view. Wide grooves separate the adjacent costae. This form differs from other species of the genus *Pseudodictyomitra* by having wide grooves separating the adjacent costae, and thin and weak costae.

Squinabollum fossilis (Squinabol, 1903)
Plate 1, Figure 19
Clistophaena fossilis Squinabol, 1903, p. 130. pl. , fig. 11.
Sethocapsa sp. A. cf. *S. simplex* Thurow, p. 405, pl. 4, fig. 23.
Squinabollum fossilis (Squinabol), Dumitrica, p. 83, pl. 19, figs. 118a-122; Taketani, 1982, p. 70, pl. 6, figs. 10a-b, 11a-b; pl. 13, figs. 10, 11; Tumanda, 1989, p. 40, pl. 7, fig. 15; pl. 8, fig. 17.
Squinabollum fossile (Squinabol), O'Dogherty, 1994, p. 203, pl. 32, figs. 4–10.

Remarks: This single specimen is not well preserved. This species refers to Dumitrica (1970).

Stichomitra communis Squinabol, 1903
Plate 1, Figures 3–5

Stichomitra communis Squinabol, 1903, p. 141, pl. 8, fig. 40; Taketani, 1982, p. 54, pl. 3, fig. 9, and pl. 11, fig. 5; Thurow, 1988, p. 406, pl. 4, fig. 10; Tumanda, 1989, p. 40, pl. 7, fig. 7; O;Dogherty, 1994, p. 144, pl. 17, figs. 6–16; Bak, 2011, p. 118, figs. 54K, L.

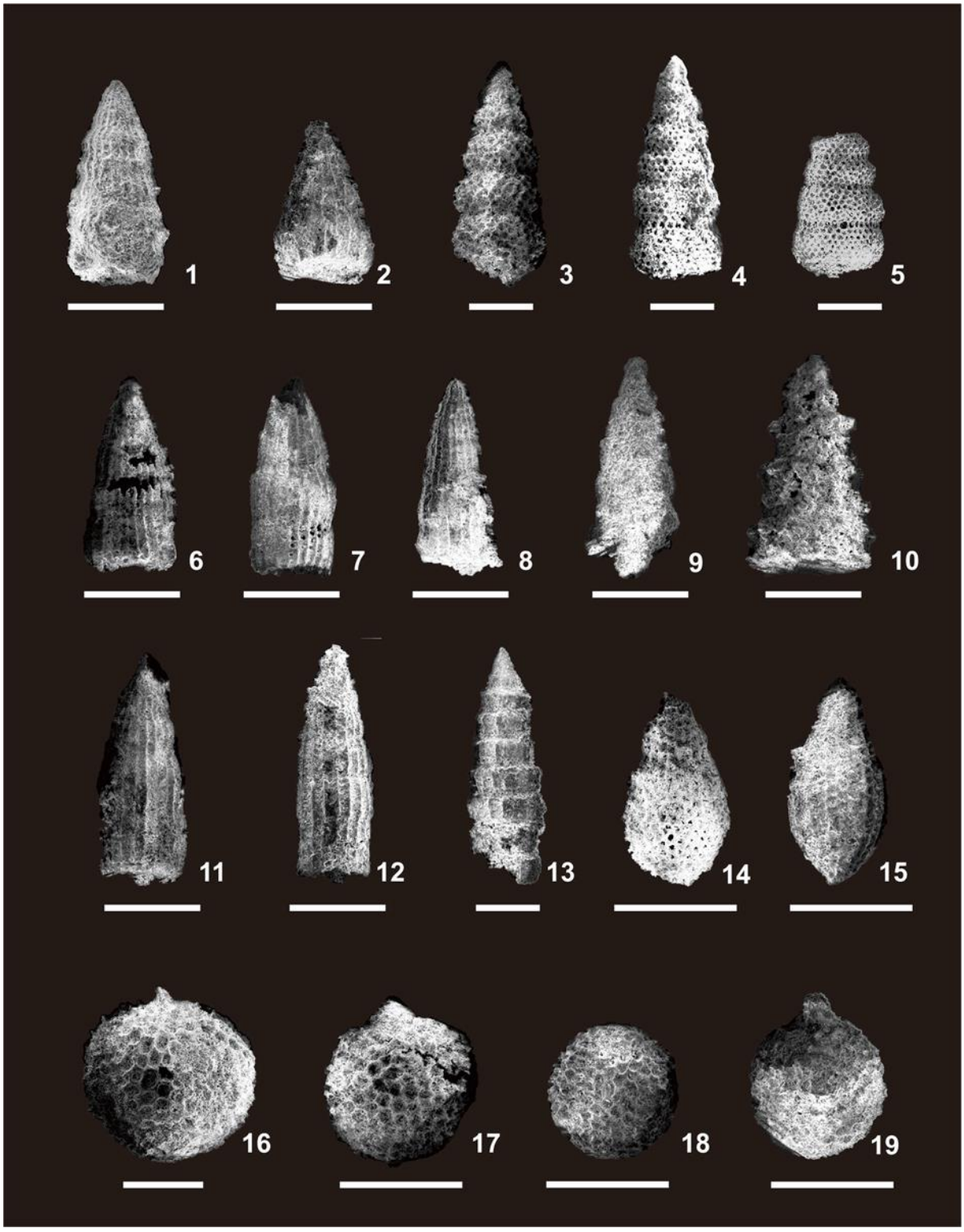


Plate 1. *Late Cretaceous radiolarians from the Noni Formation, West Timor. (1) Dictyomitra formosa. (2) Archaeodictyomitra sp. (3–5) Stichomitra communis. (6) Archaeodictyomitra sp. (7–8, 11–12) Dictymitra montisserei. (13) Pseudodictyomitra sp. A. (14) Diacanthocapsa euganea. (15) Guttacapsa biacuta. (16) Dorypyle elliptica. (17) Cryptamphorella conara. (18) Cryptamphorella sp. (19) Squinabollum fossilis. All images are scanning electron photomicrographs. Bar scales = 100μm.*

Remarks: This species is recorded from upper Cenomanian to lowermost Coniacian strata of Japan, from Cenomanian to Turonian strata of southern Europe and northwest Africa, and from Albian to Turonian strata at Hole 398D and Oman (Thurow, 1988); Albian-Cenomanian of Mediterranean region (O'Dogherty, 1994; Umbria-Marche, central Italy (Bak, 2011)).

Stichomitra sp. cf. *S. stocki* (Campbell & Clark, 1944)
Plate 1, Figure 9
Remarks: Poorly preserved specimen. Multi-segmented test, conical to cylindrical distally, with hemispherical cephalis, knob-like. We place this taxon as a form that closely resembles *Stichomitra stocki* by its general outline. *Stichomitra stocki* was re-described by O'Dogherty (1994) as a taxon that many authors subsequently identified as most typical for the genus *Amphipindax* Foreman (1966).

Novixitus sp. cf. *N. mclaughlini* Pessagno, 1977
Plate 1, Figure 10
Remarks: Poorly preserved specimen. This taxon resembles *Novixitus mclaughlini* by its general outline. Test multicyrtid, elongated, with row of large tubercles, without apical horn.

2. Suborder Spumellaria
Crucella sp.
Plate 2, Figures 6–7
Remarks: Poorly preserved specimens. Four-rayed hagiastrid. Rays equal in length, sharply pointed distally. Central area faintly raised, with central depression. This form is recorded from the Late Triassic to Late Cretaceous.

Paronaella communis (Squinabol, 1903)
Plate 2, Figures 1–2
Spongotripus communis Squnabol, 1903, p. 123, pl. 9, fig. 7.
Paronaella communis (Squinabol, 1903), O'Dogherty, 1994, p. 353, pl. 66, figs. 9–16.
Remarks: Poorly preserved specimens. Three-rayed forms having patagium. Test relatively flattened, and triangular in outline. This form is recorded from late Cenomanian to early Turonian of the Mediterranean region (O'Dogherty, 1994).

Patelulla verteroensis (Pessagno, 1963)
Plate 2, Figure 14
Stylospongia verteroensis Pessagno, 1963, p. 199, pl. 3, figs. 1–3; pl. 6. Figs. 2–3; pl. 7, figs. 3, 6.
Patellula verteroensis (Pessagno), Thurow, 1988, p. 403, pl. 2, figs. 19, 20; Tumanda, 1989, p. 34, pl. 9, figs. 15, 16; O'Dogherty, 1994, p. 328, pl. 60, figs. 25, 26; Bak, 2011, p. 146, fig. 67I.
Remarks: Test plane-convex in cross- section, circular in outline, lacking spines. This form is recorded from Campanian sediments in the Caribbean region, North Atlantic, Bavaria, and Cyprus (Thurow, 1988), and from the Turonian of the Mediterranean region (O'Dogherty, 1994).

Pessagnobrachia sp.
Plate 2, Figure 13
Remarks: This form of an incomplete specimen, is a distal part of three-rayed *Pessagnobrachia*. Tentatively, this taxon is included in the genus *Pessagnobrachia* (synonym of *Patulibrachium*) following remarks in O'Dogherty (1994).

Pessagnobrachia fabianii (Squinabol, 1914)
Plate 2, Figure 3
Rhopalastrum Fabianii Squinabol, 1914, p. 274, pl. 21, fig. 4.
Pessagnobrachia fabianii (Squinabol), O'Dogherty, 1994, p. 359, pl. 67, figs. 17–25.
Remarks: Poorly preserved specimens. Three-rayed hagiastrid. Rays relatively equal in length, and circular in cross-section. Occurs in the late Albian to early Turonian in the Mediterranean region (O'Dogherty, 1994).

Pessagnobrachia irregularis (Squinabol, 1903)
Plate 2, Figure 4
Rhopalastrum irregulare Squinabol, 1903, p. 122, pl. 9, fig. 10.
Patulibracchium inaequalum Pessagno, 1976, p. 30, pl. 1, fig. 2.
Pessagnobrachia irregularis (Squinabol), O'Dogherty, 1994, p. 360, pl. 68. Figs. 1–8.
Remarks: Form of not well preserved specimen. Three-rayed hagiastrid, with unequal interradial angles between rays. Rays very long, always unequal in length. Occurs in the middle Albian to middle Cenomanian of the Mediterranean region (O'Dogherty, 1994).

Praeconocaryomma lipmanae Pessagno (1976)
Plate 2, Figure 15
Praeconocaryomma lipmanae Pessagno, 1976, p. 41, pl. 4, figs. 12, 13; Taketani, 1982, p. 47, pl. 9, fig. 3; Bak, 2011, p. 132, figs. 60B, C.
Conocaryomma lipmanae (Pessagno), Thurow, 1988, p. 398, pl. 5, Fig. 9.
Remarks: Middle Cenomanian to Turonian of Japan, upper Cenomanian to lower Turonian of California, and upper Albian of the North Atlantic (Thurow, 1988).

Praeconocaryomma sp. cf. *P. universa* Pessagno (1976)
Plate 2, Figure 16
Remarks: Specimen is not well preserved. Cortical shell with latticed nodes possesing pore frames of variable size, close resemblance in outline to *Praeconocaryomma universa* Pessagno.

Pseudoacanthosphaera sp. cf. *P. spinosissima* (Squinabol, 1904)
Plate 2, Figures 11–12

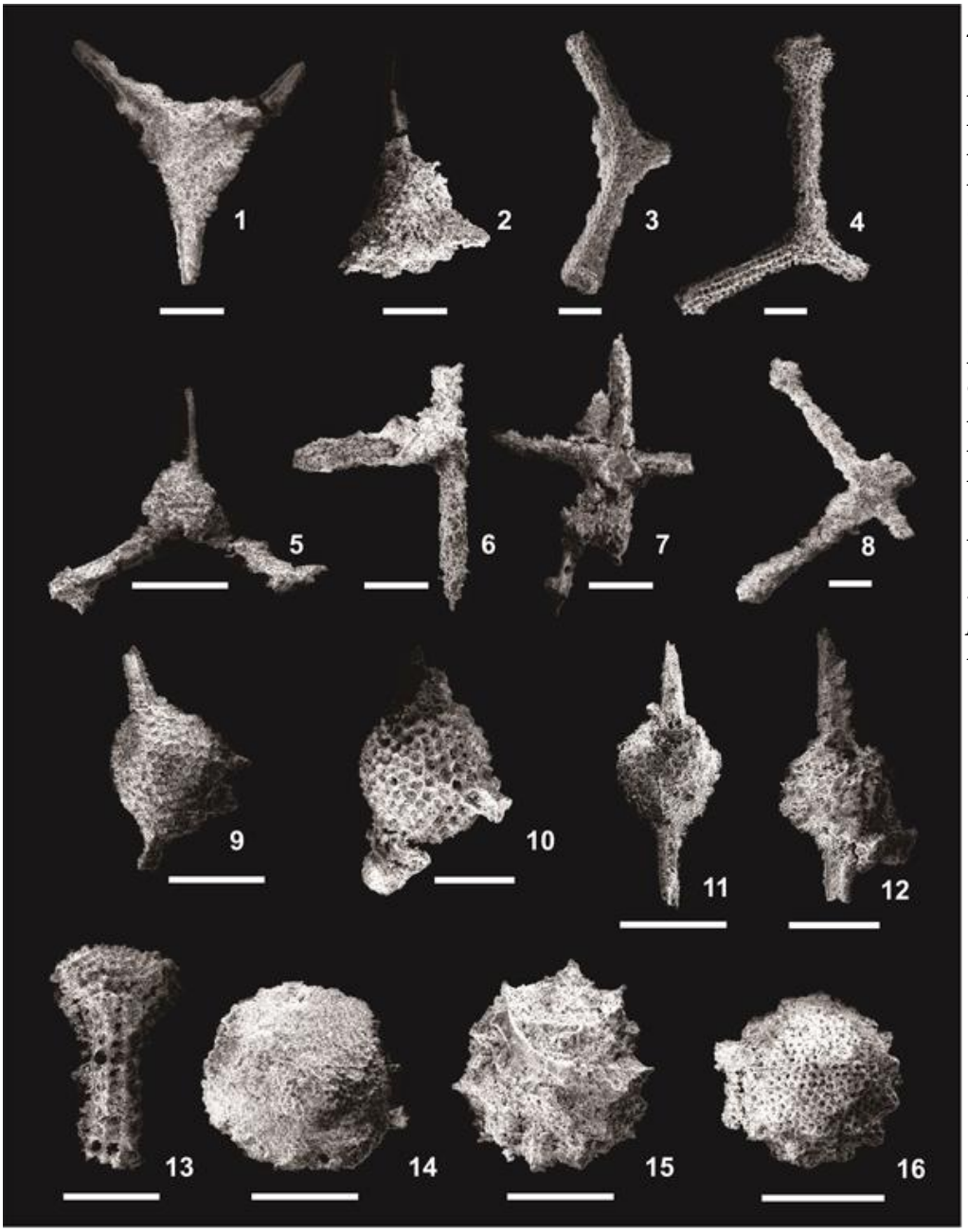


Plate 2. *Late Cretaceous radiolarians from the Noni Formation, West Timor. (1–2) Paronaella communis. (3) Pessagnobrachia fabianii. (4) Pessagnobrachia irregularis. (5) Spumellarian gen. et. sp. indet. (6–7) Crucella sp. (8) Savaryella sp. (9–10) Triactoma sp. cf. T. cellulosa. (11–12) Pseudoacanthosphaera sp. cf. P. spinosissima. (13) Pessagnobrachia sp. (14) Patelulla verteroensis. (15) Praeconocaryomma lipmanae. (16) Praeconocaryomma sp. cf. P. universa. All images are scanning electrom photomicrographs. Bar scales = 100µm.*

Remarks: Test with small spinose cortical shell and two moderately long primary spines. Primary spines with three-bladed ridges.

Savaryella sp.
Plate 2, Figure 8
Remarks: Poor preserved specimen of Hagiastrid with four spongy rays. Massive rays with rounded ray tips. This taxon is tentatively included in the genus *Savaryella* Jud (1994). Berriasian to Turonian (O'Dogherty, 1994).

Triactoma sp. cf. *T. cellulosa* Foreman
Plate 2, Figures 9–10
Remarks: Test having subspherical cortical shell, slightly triangular in outline with three bladed primary spines. Three primary spines commonly disposed at 120 degrees. Due to poor preservation, three of the primary spines are broken. Middle Albian to early Turonian in the Mediterranean region.

Spumellarian gen. et. sp. indet.
Plate 2, Figure 5
Remarks: Spongy cortical shell armed with three primary spines. Due to poor preservation, it seems a slender tiny spine is supported by a pair of sturdy primary spines.

CONCLUSIONS

1. A radiolarian fauna of the Noni Formation was extracted from chert exposed along the Noil Noni River, Miomaffo, West Timor. The fauna is characterized by *Cryptamphorella conara, Diacantocapsa euganea, Dictyomitra formosa, Dictyomitra montisserei, Guttacapsa biacuta,*

Stichomitra communis, Patelula verteroensis, Pessagnobrachia fabianii, Praeconocaryomma lipmanae and other taxa. One taxon that has not been recognized previously is P*seudodictyomitra* sp. A.

2. The radiolarian assemblage is assigned to the early Late Cretaceous (Cenomanian–Turonian, ~100.5–89.8 Ma according to the geologic timescale of the International Commission on Stratigraphy, 2019).

3. The radiolarian fauna from the Noni Formation has similar characteristic to those found in chert from the Bantimala area (Wakita et al., 1994) of South Sulawesi, both derived from a low paleolatitudinal belt, They differ from those of the Nakfunu Formation in the Kolbano area (Munasri and Sashida, 2018), the black shales and green to white radiolarian chert of Succession E of Harsolumakso et al., 1995) in South West Timor, and the thin-bedded siliceous argillites found as large blocks in mélange near Viqueque, Timor Leste (Haig and Bandini, 2013), all of which have a larger influence of "non-Tethyan fauna" and were derived from the Northern Austral Province (Southern Hemisphere) as defined by Pessagno and Hull (2002).

4. The Late Cretaceous radiolarian-bearing chert of the Noni Formation is interpreted to be deposited in the Tethyan realm or low paleolatitudinal belt, as a part of the 'allochthonous' Banda Terrane.

ACKNOWLEDGEMENTS

We thank Tim Charlton of the Timor Gap Onshore Block who provided the English improvement in the initial manuscript and offering constructive comments regarding the geology of Timor. We extend our thanks to J. T. (Han) van Gorsel of the Bibliography of Indonesian Geology who improved the quality of this paper and adding related references. The first author received a lot of suggestions from Agus Handoyo Harsolumakso. He wished to write and clarify the Stratigraphy of West Timor, but the devoted plan was not fulfilled because he passed away in Ambon on October 18th in the course of giving a geology lecture at Pattimura University. The map drawings were prepared by Indra Wahyu Perdana, an intern in the Geology Department of ITB, for that we thank.

REFERENCES

Aliev, K.S., 1965. Radiolarians of the Lower Cretaceous deposits of northeastern Azerbaidzhan and their stratigraphic significance. Izdatel'stvo Akademii Nauk, Azerbaidzhanskoi SSR, Baku, 124p. (In Russian language).

Audley-Charles, M.G., 1968. The Geology of Portuguese Timor. Geol. Soc. London, Mem. 4, 76p.

Audley-Charles, M. G., Carter, D. J. & Barber, A. J., 1974. Stratigraphic basis for tectonic interpretation of the outer Banda arc, Eastern Indonesia. *In*: Proc. Indonesian Petroleum Association, 3rd Annual Convention, p. 25-44.

Audley-Charles, M.G. & Harris, R.A., 1990. Allochthonous terranes of the Southwest Pacific and Indonesia. Philos. Trans. Royal Soc. London 331, p. 571-587.

Audley-Charles, M. G., 2011. Tectonic post-collision processes in Timor. Geological Society, London, Special Publ. 355, p. 241-166.

Bak, M., 2011, Tethyan radiolarians at the Cenomanian–Turonian Anoxic Event from the Apennines (Umbria-Marche) and the Outer Carpathians: palaeoecological and palaeoenvironmental implications. Studia Geologica Polonica 134, p. 5-279.

Bandini, A.N., Baumgartner, P.O. & Caron, M., 2006. Turonian Radiolarians from Karnezeika, Argolis Peninsula, Peloponnesus (Greece), Eclogae Geologicae Helvetiae, 99, Suplement 1, p. S1-S20.

Barber, A. J. 1979. Structural interpretation of the island of Timor, eastern Indonesia. Proc. SE Asian Petrol. Explor. Soc. 4, p. 9-21.

Barber, A. J., Audley-Charles, M. G. & Carter, D. J. 1977. Thrust tectonics on Timor. J. Geol. Soc. Australia. 24, p. 51-62.

Baumgartner, P. O., 1992. Lower Cretaceous radiolarian biostratigraphy and biogeography off northwestern Australia (ODP Sites 765 and 766 and DSDP Site 261), Argo Abyssal Plain and Exmouth Plateau. In Gradstein, F. M. et al. (eds.), Proc. of the Ocean Drilling Program, Scientific Results, College Station, TX, 123, p. 299-343.

Baumgartner, P. O., 1993. Early Cretaceous radiolarians of the Northeast Indian Ocean (Leg 123: Sites 765, 766 and DSDP Site 261): The Antarctic-Tethys connection: In Lazarus, D. and De Wever, P. (eds.), Marine Micropaleontology 21, p. 329-352.

Carter, D.J., Audley-Charles, M.G. & Barber, A.J., 1976. Stratigraphical analysis of island arc-continental margin collision in eastern

Indonesia. J. Geol. Soc. (London) 132, p. 179-198.

Campbell, A.S. & Clark, B.L. 1944b. Radiolaria from Upper Cretaceous of Middle California. Geol. Soc. Amer. Spec. Papers 57, p. 1-61.

Charlton, T.R., Barber, A.J. & Barkham, S.T., 1991. The structural evolution of the Timor collision complex, eastern Indonesia. J. Struct. Geol. 13, p. 489-500.

Charlton, et al., 2018. TIMOR GAP Onshore Block well completion report (Unpublished).

Clowes, E., 1997. Micropalaeontological analysis of the Kolbano Sequence (Jurassic to Pliocene), West Timor, and its radiolarian fauna. Ph.D. Thesis, London University, 443p.

Dumitrica, P., 1970. Cryptocephalic and Cryptothoracic Nassellaria in some Mesozoic deposits of Romania. Revue Roumaine de Géologie, Géophysique et Géographie (série Géologie), Bucharest, 14, p. 1-124.

Earle, M.M., 1983. Continental margin origin for Cretaceous radiolarian cherts in Western Timor. Nature 305, p. 129-130.

Foreman, H.P., 1966. Two Cretaceous radiolarian genera. Micropaleontology 12, 3, p. 355-359.

Foreman, H.P., 1968. Upper Maastrichtian Radiolaria of California. Spec. Pap. Palaeont. 3, p.1-82.

Haig, D.W. & Bandini, A.N., 2013. Middle Jurassic Radiolaria from a siliceous argillite block in a structural mélange zone near Viqueque, Timor Leste: Paleogeographic implications. J. Asian Earth Sciences, 75, p. 71-81.

Haile, N.S., Barber, A.J. & Carter, D.J., 1979. Mesozoic cherts on crystalline schists in Sulawesi and Timor. J. Geol. Soc. (London) 136, p. 65-70.

Harris, R., 2006. Rise and fall of the Eastern Great Indonesian arc recorded by the assembly, dispersion and accretion of the Banda Terrane, Timor. Gondwana Research 10, p. 207-231.

Harsolumakso, A.H., Villeneuve, M., Cornee, J.-J., De Wever, P., Troncheti, G., Butterlin, J., Glacon, G. & Saint-Marc, P., 1995. Stratigraphie des series paraautochtones du Sud de Timor occidental (Indonesie). Comptes Rendus del'Academie des Sciences, Series 11A (320), p. 881-888.

International Commission on Stratigraphy, 2019. International Chronostratigraphic Chart v. 2019/05, www.stratigraphy.org

Jud, R. 1994. Biochronology and systematics of Early Cretaceous Radiolaria of the Western Tethys. Mémoires de Géologie, Lausanne, 19, p. 1-147.

Keep, M., Barber, L. & Haig, D., 2009. Deformation of the Cablac Mountain Range, East Timor: an overthrust stack derived from an Australian continental terrace. Journal of Asian Earth Sciences 35, p. 150-166.

Marks, P., 1961. The succession of nappes in the western Miomaffo area of the island of Timor; a possible key to the structure of Timor. Proc. 9th Pacific Science Congress, Bangkok 1957, Geol. Geophys. 12, p. 306-310.

Martini, R., Zaninetti, L., Villeneuve, M., Cornée, J.-J., Krystyn, L., Cirilli, S., De Wever, P., Dumitrica, P., & Harsolumakso, A., 2000. Triassic pelagic deposits of Timor: paleogeographic and sea-level implications. Palaeogeography, Palaeoclimatology, Palaeoecology 160, p. 123-151.

Munasri, 1998. Early Cretaceous radiolarian biostratigraphy of the Kolbano area, West Timor, Indonesia. Ph.D. Thesis, University of Tsukuba, Japan, (Unpublished).

Munasri and Sashida, K., 2018, Tethyan and non-Tethyan Early Cretaceous radiolarians from the Kolbano area, West Timor, Indonesia. Earth Evolution Sciences 11, p. 3-12.

O'Dogherty, L., 1994. Biochronology and paleontology of Mid-Cretaceous radiolarians from Northern Apennines (Italy) and Betic Cordillera (Spain). Mémoires de Géologie Lausanne, 21, p. 1-411.

Pessagno Jr., E.A., 1963. Upper Cretaceous Radiolaria from Puerto Rico. Micropaleontology, 9, 2, p. 197-214.

Pessagno Jr., E. A., 1976. Radiolarian zonation and stratigraphy of the Upper Cretaceous portion of the Great Valley Sequence, California Coast Ranges. Micropaleontology, Special Publ. 2, p. 1-95.

Pessagno Jr., E. A., 1977. Lower Cretaceous radiolarian biostratigraphy of the Great Valley Sequence and Franciscan Complex, California Coast Ranges. Cont. Cushman Found. Foram. Res., Spec. Publ., 15, p. 1-87.

Pessagno Jr., E. A. & Hull, D. M., 2002. Upper Jurassic (Oxfordian) Radiolaria from the Sula Islands (East Indies): Their taxonomic, biostratigraphic, chronostratigraphic, and paleogeographic significance, Micropaleontology, 48, 3, p. 229-256.

Pessagno Jr., E. A. & Newport, R. L., 1972. A technique for extracting radiolaria from radiolarian cherts, Micropaleontology, 18, 2, p. 231-234.

Sanfilippo, A. & Riedel, W.R., 1985. Cretaceous Radiolaria. *In*: Bolli, H.M., Saunders, J. B. & Perch-Nielsen, K. (eds.): Plankton Stratigraphy, Cambridge University Press, Cambridge/ New York, p. 573-630.

Sashida, K., Adachi, S., Ueno, K., & Munasri, M., 1996. Late Triassic radiolarians from Nefokoko, West Timor, Indonesia. *In*: H. Noda and K. Sashida (eds): Professor Hisayoshi Igo, commemorative volume on geology and paleontology of Japan and Southeast Asia, Tokyo: Gakujyutsu Tosho Insastsu, p. 225-234.

Sashida, K., Munasri, Adachi, S. & Kamata, Y., 1999a. Middle Jurassic radiolarian fauna from Rotti Island, Indonesia. J. Asian Earth Sciences 17, p. 561-572.

Sashida, K., Kamata, Y., Adachi, S. & Munasri, M., 1999b. Middle Triassic radiolarian faunas from West Timor, Indonesia. J. Paleontology, 73, p. 765-786.

Sopaheluwakan, J., 1990. Ophiolite obduction in the Mutis Complex, Timor, Eastern Indonesia: An example of inverted, isobaric, medium-High Pressure metamorphism. Ph.D. Thesis, Free University, Amsterdam, 226p.

Squinabol, S., 1903. Le Radiolarie dei noduli selciosi nella Scaglia degli Euganei. Contribuzione I. Rivista Italiana Paleont.9, p. 105-151.

Squinabol, S., 1904. Radiolarie cretacee degli Euganei. Atti Mem. r. Accad. Sci. Lett. Arti Padova, n. Ser., 20, p. 171–244.

Squinabol, S., 1914. Contributo alla conoscenza dei Radiolarii fossili del Veneto. Appendice - Di un genera di Radiolari caratteristico del Secondario. Mem. 1st. geol. r. Univ. Padova, 2, p. 249-306.

Taketani, Y. 1982. Cretaceous radiolarian biostratigraphy of the Urakawa and Obira areas, Hokkaido. Sci. Rep. Tohoku Univ. 52, 1-2, p. 1-75.

Tan, S.H. 1927. Over de samenstelling en het onstaan van krijten mergel-gesteenten van de Molukken. In: Brouwer, H.A. (Ed.). Jaarboek van het mijnwezen in Nederlandsch Oost-Indie 55 (1926),Verhandelingen, 3, p. 5-165.

Tappenbeck, D., 1940. Geologie des Mollogebirges und einger benachbarter Gebiete (Niederlandisch Timor). In: Brouwer, H.A. (Ed.), Geological Expedition of the University of Amsterdam to the Lesser Sunda Islands in the South Eastern Part of the Netherlands East Indies 1937, 1, N.V. Noord-Hollandsche Uitgevers Maatschappij, Amsterdam, p. 1-105.

Thurow, J., 1988. Cretaceous radiolarians of the North Atlantic Ocean: ODP Leg 103 (Sites 638, 640 and 641) and DSDP Legs 93 (Site 603) and 47B (Site 398). *In*: Boillot, G., Winterer, E.L. et al. (eds.): Proc. Ocean Drilling Program, Scientific Results, 103, College Station, TX, p. 379-418.

Tumanda, F., 1989. Cretaceous radiolarian biostratigraphy in the Esashi Mountain area, Northern Hokkaido, Japan. Sci. Rep. Inst. Geosci. Univ. Tsukuba, 10, p. 1-44.

Van West, F.P., 1941. Geological Investigations in the Miomaffo region (Netherlands Timor). In: Brouwer, H.A. (Ed.), Geological Expedition of the University of Amsterdam to the Lesser Sunda Islands in the South Eastern part of the Netherlands East Indies 1937, 3, N.V. Noord-Hollandsche Uitgevers Maatschappij, Amsterdam, p. 1-131.

Wakita, K., Munasri & Bambang, W. 1994. Cretaceous radiolarians from the Luk Ulo Melange Complex in the Karangsambung area, central Java, Indonesia. J. Southeast Asian Earth Sci., 9, 1-2, p. 29-43.

Wakita, K., Munasri, Sopaheluwakan, J., Zulkarnain, I. & Miyazaki, K., 1994. Early Cretaceous tectonic events implied in the time-lag between the age of radiolarian chert and its metamorphic basement in the Bantimala area, South Sulawesi, Indonesia. The Island Arc, 3, p. 90-102.

A New Insight of Talang Akar Formation in the Ridho Field, North Palembang Sub-basin, Indonesia: An Integrated Approach

Togi Y. Sitinjak[1#], Ricky A. Tampubolon[1], Ardian Pratama[1], Wildanto P. Nusantara[1], Aziza Muis[1] and Harsanti Setiani[2]

[1]Subsurface, Odira Energy Karang Agung Ltd, Jakarta, Indonesia
[2]PT. Geoservices Indonesia, Jakarta, Indonesia
[#]Corresponding author: togi.y@odiraka.co.id

ABSTRACT

The synrift sandstone deposits of Eo-Oligocene Lemat (LMF) and Oligo-Miocene Talang Akar Formations (TAF) are the most well-known hydrocarbon reservoirs in the South Sumatra Basin, Indonesia. However, only limited studies on TAF in the North Palembang Sub-Basin have been published. In the Ridho field, TAF is characterized by fining-up sequences of inter bedded, fine to medium-grained sandstones and shales overlain by a coal layer as the top marker, while LMF comprises of continuous blocky-shaped, medium to coarse-grained, conglomeratic sandstones.

Previous lithostratigraphy-driven sand to sand correlation between wells has created difficulties in understanding the geology and in producing consistent correlation, especially within the TAF. In order to define chronostratigraphy-based correlation and interpret the depositional environment of TAF and LMF, an integration between palynological, core study and petrophysical analysis was performed. The result of this integrated approach demonstrates aligned hypotheses. The occurrence of pollen Meyeripollis naharkotensis and Florschuetzia trilobata along the studied wells suggest Late Oligocene age. The palynology study subdivides TAF into three backmangrove-intertidal sand units with an increase of marine influence defining a transgression to the top of the TAF. The transgressive event is identified in core sample by lesser tidal influx sedimentary structures such as ripple, mudlayer, flaser and also finer grained sandstone at the top of TAF. Furthermore, based on petrophysical evaluation, better sand quality with lower NTG (net-to-gross) near top TAF confirms the retrogradational event in this formation.

The new sand unit definitions from the current study provide more consistent correlation in terms of sand thickness and characteristics for future modeling purposes.

Keywords: Talang Akar Formation, North Palembang Sub-Basin, South Sumatra Basin

INTRODUCTION

Background

The South Sumatra Basin is located on the southern part of Sumatra Island. It is bounded from Central Sumatra Basin to the north by Bukit Tiga Puluh Mountain and from Sunda Basin to the south by Lampung High. South Sumatra Basin consists of four sub-basins, namely: Jambi, Central Palembang, North Palembang, and South Palembang Sub-basins (Figure 1).

Ridho field in the North Palembang Sub-basin was discovered in 2009. Since its discovery, Talang Akar and Lemat Formations have been the main producing zones with a total production of approximately 160 MBOE from three wells. In total, six wells have been drilled in the Ridho structure, with four of them being active producers, while the rest are water injectors. Recent development activities of the field are currently progressing in order to enhance production and find more upside potentials. One of these development activities is updating the reservoir model that was previously done under the POD project in 2009. The updated reservoir model will later be used as the basis to propose drilling additional development wells.

The POD version of Ridho field's reservoir model utilized geological data that were acquired from the first two wells in the field, which consist of R-1 and

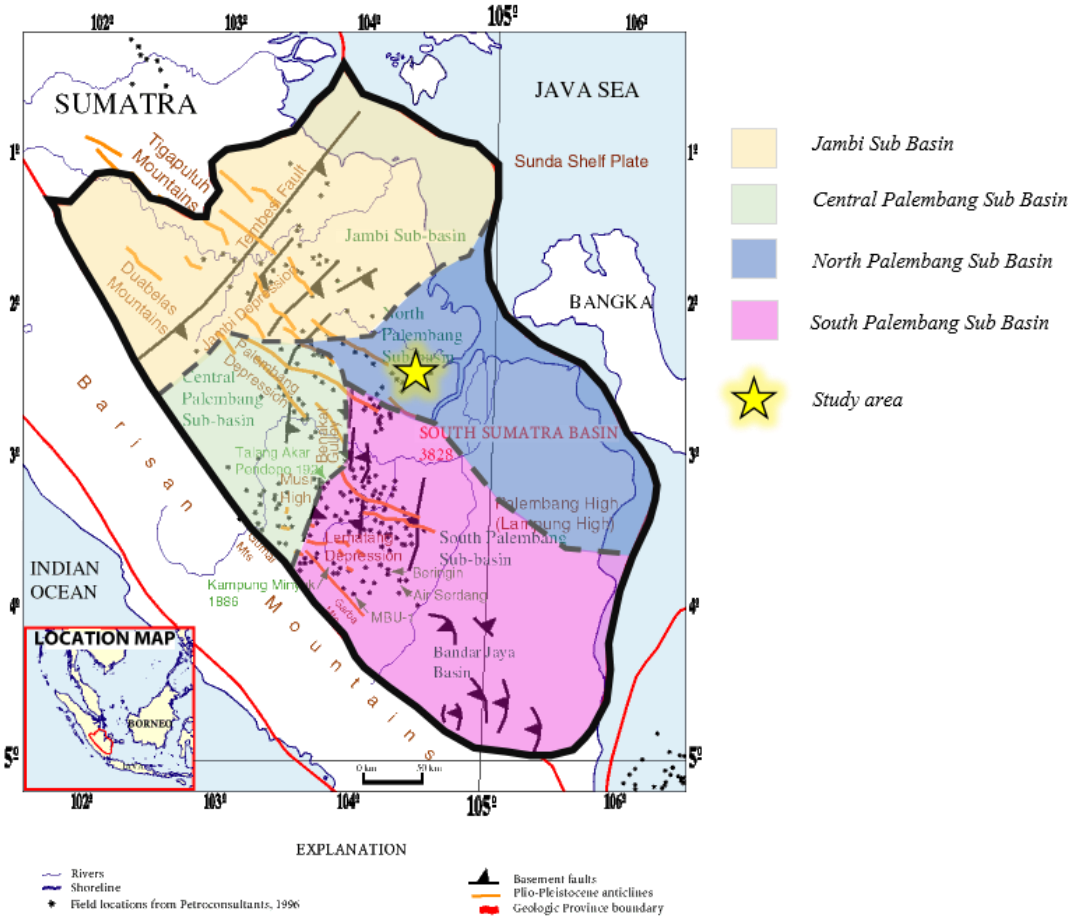


Figure 1: *Index map of the South Sumatra Basin Province, showing major structural features. The structures were assembled from Hutchinson (1996); Williams et al. (1995); Moulds (1989); van Bemmelen (1949) [after Bishop, 2001]. Highlighted yellow star is location of the current study.*

R-6. The data includes well correlation, petrophysical evaluation, and facies modeling. The more recently updated reservoir model incorporates data from four new development wells. These data consist of wireline logs, cores, and lab analyses such as palynology, RCA (Routine Core Analysis) and SCAL (Special Core Analysis).

One of the primary inputs to reservoir modeling is facies modeling based on sand to sand correlation between wells. Previous facies model (the POD version) was built by employing lithostratigraphy-based sand correlation. This lithostratigraphy technique correlates sand to sand in each well based on similarities in wireline log characters (e.g. Gamma Ray-GR, Resistivity, Density-RHOB and Neutron-NPHI logs) and also similarities in lithology composition from cuttings and core description. This technique sometimes can lead to confusion or mis-interpretation. For instance, a look-a-like sand across the wells is later proven disconnected pressure-wise, or in other words, it is not the same sand body as expected from the initial correlation. Another disadvantage of lithostratigraphy correlation is that it doesn't show the effect of geological evolution such as sea level change to the sedimentary process and reservoir quality (Nichols, 2009), which is very critical to consider when making a comprehensive reservoir model. OEKA's internal subsurface team then initiated the current study, which integrates palynological, petrophysical and core analysis data to create a chronostratigraphic sand to sand correlation and obtain deeper geological understanding on Talang Akar and Lemat Formations.

GEOLOGICAL SETTING & SEDIMENTATION HISTORY

South Sumatra Basin has undergone three major tectonic events (Suhendan, 1984), which consist of:

1. Extension during late Paleocene to early Miocene forming north-trending grabens that were filled with Eocene to early Miocene deposits (40-29 Ma);

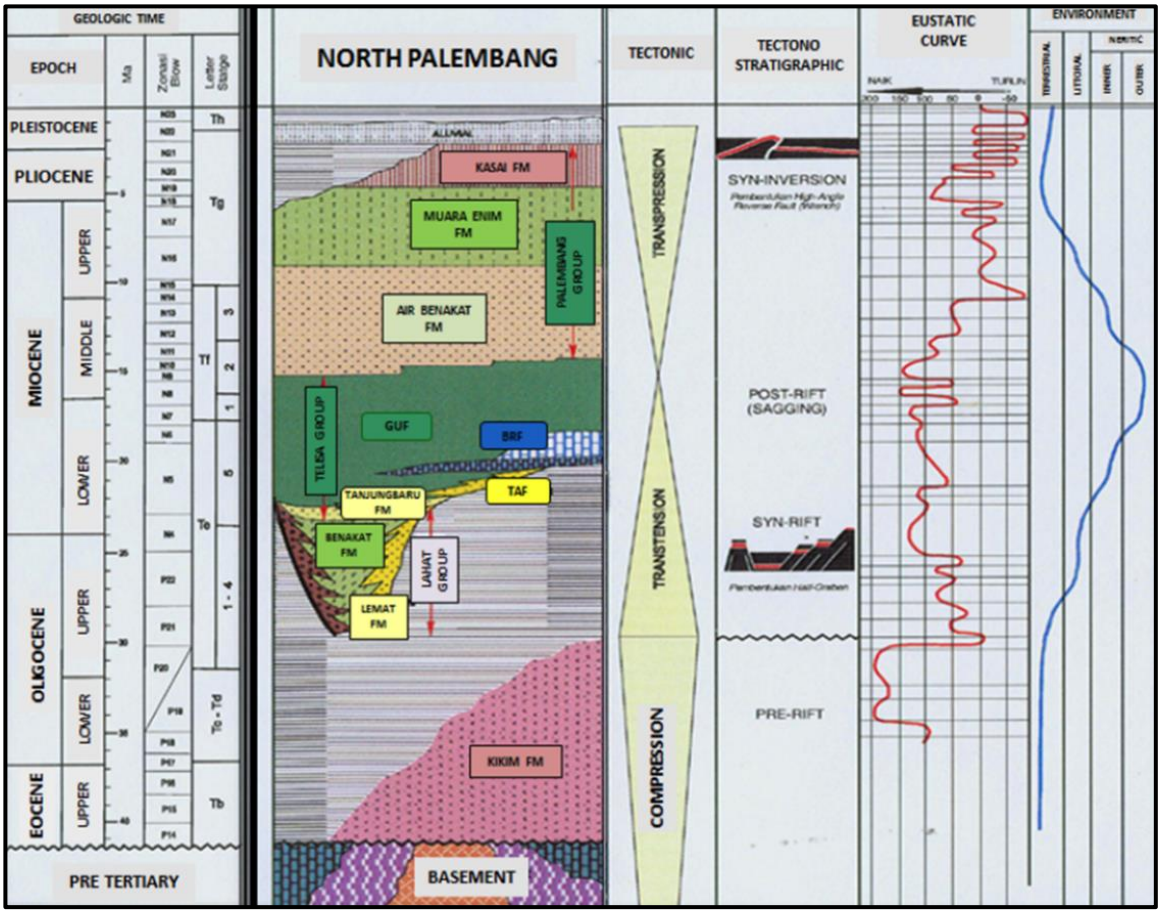


***Figure 2**: Stratigraphic column of North Palembang Sub-basin, South Sumatra Basin. (modified from Syaifudin et al., 2015)*

2. Relative quiescence with late normal faulting from early Miocene to early Pliocene (29-5 Ma); and
3. Basement-involved compression, basin inversion, and reversal of normal faults in the Pliocene to Recent forming the anticlines (5 Ma-Recent) that form major traps in the area.

Sedimentation history in the South Sumatra basin began with the deposition of continental sediments derived from local erosion of Lemat Formation in the Eocene (Cole and Crittenden, 1997; Courteney et al., 1990). As the rifting phase weakened during late Oligocene time, transgression occurred as a result of thermal sag and eustatic gain (Netherwood, 2000; Barber et al., 2005). This transgression event was then followed by sedimentation of Talang Akar Formation in several rifted grabens. The sediments of Talang Akar Formation were deposited in various depositional settings, from fluvial to deltaic and drives mixed sediment strata consisting of interbedded sandstones, shales, and coals. In the earliest Miocene, as the transgression continued, the depositional settings of Talang Akar Formation changed gradually from fluvial to more deltaic and then marginally-deep marine.

During the Early Miocene, deposition of Baturaja Formation flourished on structural highs as carbonate buildups on some local inter-graben highs and basin margins or as carbonate mud-dominated in the low energy banks (Situmeang et al.,1992; Longman et al., 1992). In the deeper part of the basin, a shale-dominated strata with thinly bedded sandstone and limestone intercalation, Gumai Formation, was deposited. During the Middle Miocene's maximum transgression, the Gumai shale seal across the region creating the most widespread regional seal (De Coster, 1974).

In the Middle Miocene, development of the Barisan Mountains and possible volcanic islands to the south and southeast, further decreased and then cut off and overwhelmed marine influences and added new clastic and volcaniclastic sources from those directions (De Coster, 1974; Cole and Crittenden, 1997; Hamilton, 1979).

Deposition during the Middle Miocene-Pliocene compressional regimes started with shallow marine

– deltaic Air Benakat and Muara Enim Formations. Air Benakat Formation consists mainly of sandstone and fine-grained siliciclastic rocks, while coal bed intercalations occur in the Muara Enim Formation.

In the Pliocene, the sedimentation was driven mainly from the west and northwest of the basin which marked the Kasai Formation deposition. This formation overlies the Muara Enim Formation unconformably and consists of conglomerates, tuffaceous sandstone, and tuffs with lignite and silicified wood.

METHODS

This study integrates palynological, petrophysical and core interpretation. Palynological analysis was performed on fifty-four (54) ditch cutting samples from five (5) Ridho wells. These samples picks were based on high Gamma Ray readings. The sample list for palynological analysis is shown in Table 1.

These samples were then utilized for palynological slide preparation. The slides were examined under the microscope for palynological content. Quantitative palynology analyses were carried out for this study. One palynological slide was examined in detail and the palynomorphs were counted. The actual number of specimens of rarer species was counted on the slide and was recorded. Where yields were lean, the total number of specimens on the slide was provided. Fungal palynomorph counts were recorded, but these are complimentary to the standard counts.

In addition to the palynomorphs counts, a visual estimate of the relative proportions of the palynomacerals and structureless organic matter (SOM) was made from the kerogen slide. The identification of these kerogen components broadly follows techniques described by Van der Zwan (1990) and Whitaker et al. (1992). The palynological classification applied is summarized and the main palynomaceral types are described in more details.

Table 1. *Palynological analysis samples of Ridho field.*

Well	Palynology			Samples depth (mMD)
	Ditch Cuttings (#samples)	Sidewall Cores (#samples)	Core (#samples)	
R-1	13	0	0	1318-1320; 1322 – 1324; 1332-1334; 1338-1340; 1346-1348; 1356 – 1358; 1358-1360; 1370-1372; 1372-1374; 1380-1382; 1440-1442; 1442-1444; 1452-1454
R-2	11	0	0	1324-1326; 1338-1340; 1348 – 1350; 1356 – 1358; 1372 – 1374; 1388 – 1390; 1404 – 1406; 1414 – 1416; 1432 – 1434; 1458 – 1460; 1470 - 1472
R-3	10	0	0	1314 – 1316; 1328 – 1330; 1334 – 1336; 1348 – 1350 1362 – 1364; 1374 – 1376; 1388 – 1390; 1394 – 1396 1400 – 1402; 1442 – 1444
R-4	10	0	0	1348 – 1350; 1362 – 1364; 1374 – 1376; 1402 – 1404 1410 – 1412; 1420 – 1422; 1438 – 1440; 1444 – 1446 1456 – 1458; 1494 – 1496
R-5	13	0	0	1344 – 1346; 1348 – 1350; 1368 – 1370; 1374 – 1376 1384 – 1386; 1400 – 1402; 1402 – 1404; 1408 – 1410 1428 – 1430; 1438 – 1440; 1444 – 1446; 1490 – 1492 1492 – 1494
Totals	**57**	**0**	**0**	

For petrophysical analysis and core interpretation, well data such as wireline logging, core analysis data (RCAL and SCAL reports), mudlogging and PVT analysis from 6 (six) wells were utilized. The complete lists of well data are shown in Table 2.

The textural parameters (a-tortuosity constant, m-cementation factor, and n-saturation exponent) for petrophysical evaluation were taken from special core analysis (SCAL). The result obtained from SCAL analysis are shown in Table 3.

Formation water salinity for petrophysical evaluation was measured from PVT-Ten Ion water analysis. The Rw from the measurement is 0.34 ohmm at 75°F (~16.6 k ppm NaCl).

Standard deterministic petrophysical evaluation was carried out in this study. First, QC and environment correction for all the wireline log were performed. Second, petrophysical parameters such as Vsh, Phi, and Sw, were calculated from the wireline logs. Third, cutoff Vsh, PHIE, and Sw were applied to define net sand, net reservoir and net pay. Finally, all the calculated petrophysical parameters were calibrated with the core data, and the estimated net pay zone was validated with perforation zone.

***Table 2**. Well data availability of Ridho field*

Well	LAS	CALI	GR	SP	LLD	MSFL	RD	RMLL	RS	RHOB	ZDNC	NPHI	CNCF	DT	PEF	JPEG
R-1	✓	✓	✓	✓	✓	✓				✓		✓		✓	✓	✓
R-2	✓	✓	✓	✓			✓	✓	✓		✓		✓	✓	✓	✓
R-3	✓	✓	✓				✓	✓	✓		✓		✓	✓	✓	
R-4	✓	✓	✓	✓			✓	✓	✓		✓		✓	✓	✓	✓
R-5	✓	✓	✓	✓			✓	✓	✓		✓		✓	✓	✓	✓
R-6	✓	✓	✓	✓	✓	✓				✓		✓		✓	✓	✓

Well	Cutting	Mudlog/ Composite Log	Well Report	RCAL	SCAL	SWC	Geochem	PVT Ten Ion	Status
R-1	✓	✓	✓	✓	✓	✓			Oil Producer
R-2	✓	✓	✓	✓			✓	✓	Oil Producer
R-3	✓	✓	✓				✓	✓	Oil Producer
R-4	✓	✓	✓	✓			✓	✓	Injector
R-5	✓	✓	✓	✓			✓	✓	Oil Producer
R-6	✓	✓	✓	✓	✓	✓			Injector

***Table 3**. SCAL analysis for a, m, and n factor.*

Well	a	m	n	No. of Samples	#Sample No. - Depth (mMD)
R-2	1	1.98	1.8864	3	#4 (1389.9) #11 (1392.92) #25 (1397.35)
R-3	1	1.98	1.8685	3	#1 (1403.15) #18 (1409.11) #27 (1410.86)
R-4	1	1.98	1.8730	3	#5 (1401.06) #8 (1401.9) #17 (1404.12)

Core interpretation was done by plotting the core image in their corresponding depth and by logging and describing all the sedimentary structures, a change in grain size, and by identifying parasequence to create the geological interpretation. It is critical to validate the core depth if any misfit occurred. This was done by comparing depth of the core's Gamma vs the wireline's Gamma Ray curves. Beside the geological structures, other RCAL measurements such as porosity, permeability, and lithology description were used as supporting data to build geological interpretation.

RESULT

POD Sand to Sand Correlation Overview

Based on POD report of the Ridho Field, the sand units of Talang Akar and Lemat Formations were subdivided into three sand bodies including TAF SS-1, TAF SS-2, and Lemat-SS. The top and bottom of each sand units were defined based on the characters of the conventional wireline logs that encompasses GR, Resistivity, and Density-Neutron from R-1 and R-6 wells. Figure 3 exhibits the lithostratigraphy sand to sand correlation of R-1 and R-6 wells.

Table 4 shows the thickness of each sand body. As shown in Table 4, Sand TAF SS-2 is thickening to R-6 well while other sands seem to have quite consistent thickness between the two wells. Based on Figure 3, it is quite clear that the division of sand body can still be fine-tuned especially on TAF SS-2 as some shale breaks may separate the TAF SS-2 sand into different individual sands.

As more wireline data are available from 5 (five) additional development wells, the sand to sand correlations are updated with reference to R-1 and R-6 correlation. There are some justifications made to change sand bodies definition. Two (2) new sand bodies, TAF A1 and TAF A2, are introduced as the upper most sand body in the TAF. While, TAF SS-2 is sub-divided into three separated sand bodies TAF SS-2, TAF SS-3, and TAF SS-4. Figure 4 depicts the updated well correlations. The total gross thickness of each sand is shown in Table 5.

The gross thickness of each sand is inconsistent from well to well. Another strange finding from these tops picking is the significant thickness change of Lemat SS in R-2 well compared to those in other wells. This inconsistency rises an uncertainty on the sand unit definition for further modeling.

Palynology Analysis Result

Palynological analyses generally provide main information such as age and depositional environment. These information were taken based on the organic material or macerals presence in a sample, which may comprise: (1) wood, leaf and associated plant debris, (2) spores and pollen derived from plants which inhabit the land or freshwater, (3) pollen derived from plants that can tolerate brackish water, including mangroves, (4) algal cysts derived from freshwater, brackish and marine environments, (5) other organic-walled organisms including certain foraminifera. The individual occurrences, associations and relative abundances of the major fossil groups of various types of palynomorphs provide indications of the various depositional regimes and any changes from one depositional regime to another.

Three age markers are recognized based on palynology analysis in which all the markers predominantly correspond to Late Oligocene with very minor Early Miocene spores. These three time markers represent FDO (First Downhole Occurrence) of the fossil spores *Meyeripollis naharkotensis*, Peak or Acme of *Meyeripollis naharkotensis* and FDO of *Cicatricosisporites dorogensis*. The complete result of the pollen is shown in Table 6.

***Table 4**. Gross thickness of each sand body as defined in POD report of the Ridho field.*

Well	Sand Body	Top (mTVDSS)	Bottom (mTVDSS)	Gross Thickness
R-1	TAF SS-1	1311.35	1319.19	7.84
R-1	TAF SS-2	1327.72	1363.04	35.32
R-1	Lemat SS	1371.54	1403.56	32.02
R-6	TAF SS-1	1321.83	1329.62	7.79
R-6	TAF SS-2	1335.15	1375.55	40.4
R-6	Lemat SS	1382.95	1415.95	33

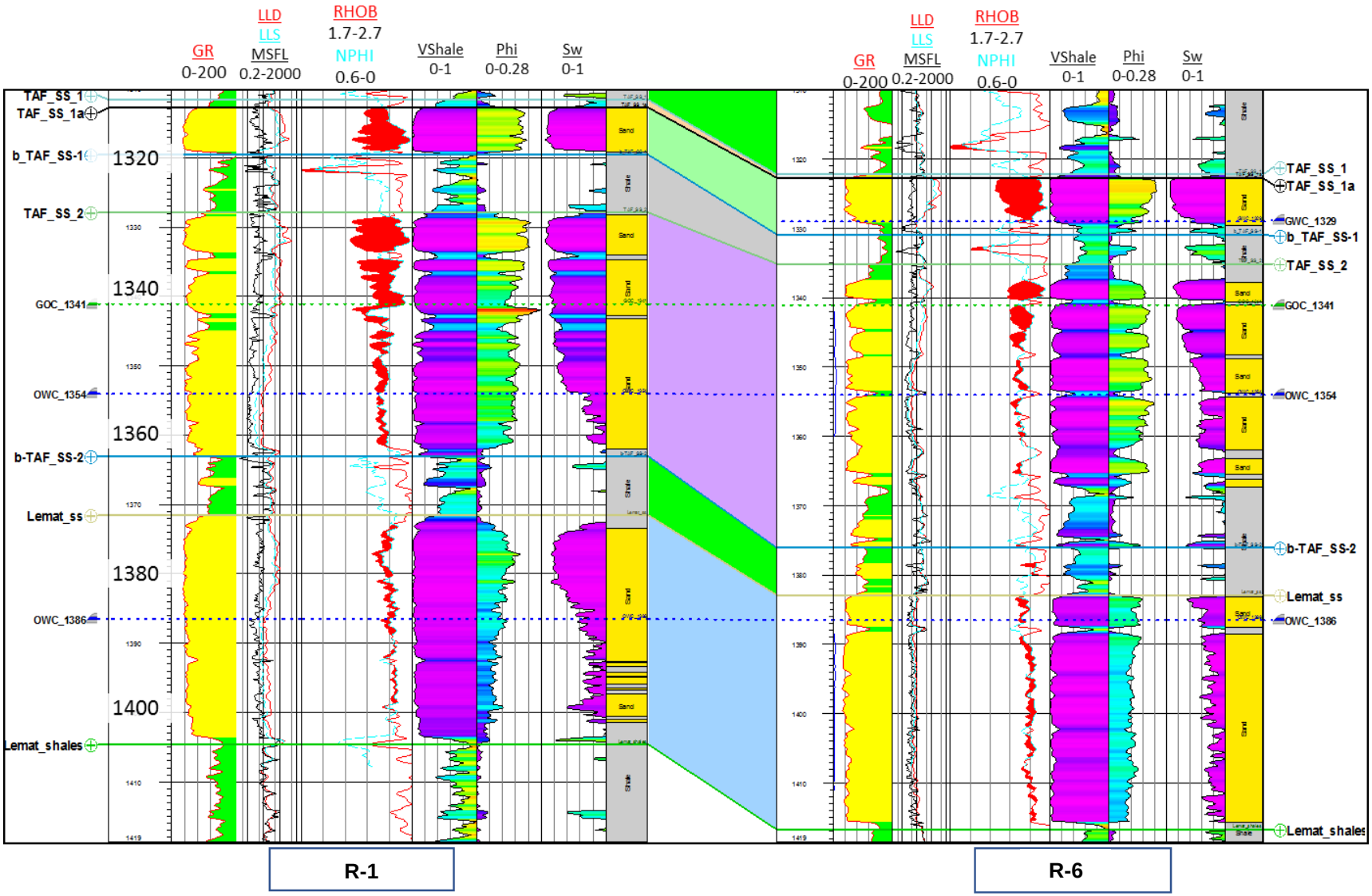


***Figure 3**: Lithostratigraphy correlation of R-1 and R-6 wells (plotted on TVDSS).*

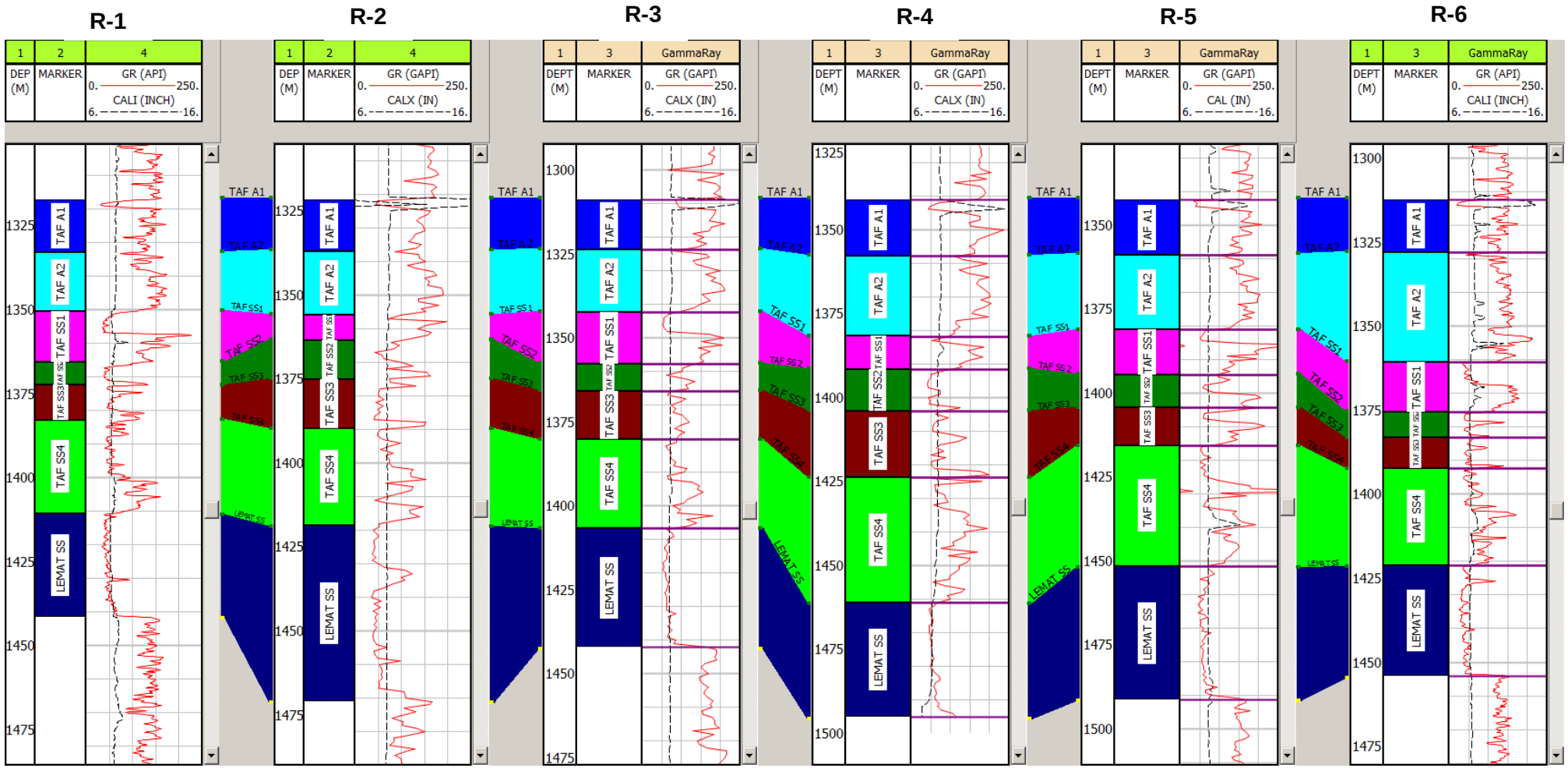


Figure 4: *Well correlation showing lithostratigraphy of the Ridho Field.*

***Table 5**. Gross thickness of TAF and Lemat SS based on Ridho wells.*

Well	Formation Tops (metres) (Gross Thickness)						
	TAF A-1	**TAF A-2**	**TAF SS-1**	**TAF SS-2**	**TAF SS-3**	**TAF SS-4**	**Lemat-SS**
R-1	1317.31 *(15.78)*	1333.09 *(17.46)*	1350.55 *(15.08)*	1365.63 *(6.88)*	1372.51 *(10.34)*	1382.85 *(28.04)*	1410.89 *(30.76)*
R-2	1321.68 *(15.27)*	1336.95 *(19.07)*	1356.02 *(7.42)*	1363.44 *(11.65)*	1375.09 *(14.72)*	1389.81 *(28.8)*	1418.69 *(52.28)*
R-3	1308.90 *(14.98)*	1323.88 *(18.52)*	1342.40 *(15.29)*	1357.69 *(8.15)*	1365.84 *(14.5)*	1380.34 *(26.32)*	1406.66 *(35.52)*
R-4	1341.14 *(16.84)*	1357.98 *(23.99)*	1381.79 *(9.61)*	1391.58 *(12.43)*	1404.01 *(19.85)*	1423.86 *(37.3)*	1461.16 *(33.97)*
R-5	1342.55 *(16.37)*	1358.92 *(22.36)*	1381.28 *(13.28)*	1394.56 *(9.89)*	1404.45 *(11.26)*	1415.71 *(35.96)*	1451.67 *(39.69)*
R-6	1312.35 *(15.73)*	1328.09 *(32.55)*	1360.63 *(14.82)*	1375.45 *(7.67)*	1383.12 *(9.26)*	1392.38 *(28.92)*	1421.30 *(32.80)*

***Table 6**. Age/zonation markers of Ridho field wells.*

Age/ Zonation	Comment	Well Name				
		R-1	**R-2**	**R-3**	**R-4**	**R-5**
?Early Miocene/ ?*F. trilobata*	This zone assigned based stratigraphic position above the FDO of *Meyeripollis naharkotensis* and *Cicatricosisporites dorogensis* and the presence of *F. trilobata.*	-	1326 (FSE) - 1340	-	-	-
Late Oligocene/ *M. naharkotensis*	The FDO of *Meyeripollis naharkotensis* at this interval may suggest the penetration of Oligocene age. This is supported by the presence of *Cicatricosisporites dorogensis.* The presence of *Proxapertites operculatus* at this interval interpret as reworked taxa from Eocene interval.	1320 (FSE) - 1358	1350 - 1358	1316 - 1444	1350 - 1496	1346 - 1494
	Peak *Meyeripollis naharkotensis*: This level recognized by the most abundant *M. naharkotensis.*	1360	1374	1364	1422	1386

***Table 7**. Chronostratigraphic unit definition in present study. (UTAF-Upper Talang Akar; LTAF-Lower Talang Akar; ULMF-Upper Lemat).*

Sand Unit	Top Marker	Bottom Marker	Well Top Depth (mMD)				
			R-1	R-2	R-3	R-4	R-5
UTAF-2	Coal Marker	FDO *Meyeripollis naharkotensis/ F.Trilobata*	1317	1321	1308.1	1341	1342.2
UTAF-1	FDO *Meyeripollis naharkotensis/*	Peak/Acme of *Meyeripollis naharkotensis*	1346	1348	1334.2	1364	1373.7
LTAF-2	Peak/Acme *Meyeripollis naharkotensis*	FDO *Cicatricosisporites dorogensis.*	1358	1372	1362	1422	1386
LTAF-1	FDO *Cicatricosisporites dorogensis.*	LDO *Cicatricosisporites dorogensis/* FDO *P.Kutchensis*	1380	1404	1388	1446	1437.6
ULMF-2	LDO *Cicatricosisporites dorogensis/* FDO *P.Kutchensis*	Bottom Lemat SS	1411	1436	1406.7	1461.2	1451.7

Based on the age marker from palynology analyis, new chronostratigraphic sand units were introduced. These new sand units are given in Table 7.

From the analyzed palynological slides, 90 palynomorphs species were identified. Twelve were fungal spore, 17 were pteridophytes and 47 were land angiosperm, 5 were mangrove plantation, 8 were back mangrove plantation and 1 was dinoflagellate cyst. The pollen facies interpretation example for R-1 is demonstrated in Figure 5. The complete palynofacies analysis for the other wells are presented in the appendices.

Petrophysical Analysis Result

The new top and bottom of the sand units replaced prior lithostratigraphy sand unit and were used in the subsequent petrophysical evaluation. The sand unit's NTG, Porosity, Vsh and Sw for each sand unit are shown by histogram in Figure 6. One can observe a relatively higher NTG in Lemat compared to that in the LTAF and UTAF. While from the Vsh and PHIE for reservoir layers, all the sand units can be categorized as a good-very good sand with maximum Vsh reservoir < 0.3, PHIE > 0.15. Unlike the NTG, the reservoir Vsh and PHIE show opposite trend where UTAF and LTAF possess better PHIE and Vsh. As R-4 is an injector well and structurally lower, the Sw of this well is the lowest compared to other wells, the vice versa can be seen in R-3.

The permeability are calculated by finding relationship between the core porosity and core permeability from RQI (Rock Quality Index) methods which is out of the scope of this publication. This method is used to generate the rock facies classifications.

The well section in Figure 8 exhibits petrophysical evaluation of the Ridho field wells (only producer wells are shown).

Core Interpretation

Figure 9 shows photograph of a core taken from a well that penetrated Lower Talang Akar Formation. Common features of the cores from this formation include:

- Pebbly sandstone at the base of parasequence, showing a lag deposit
- Common rock fragments indicating the sediment source is near
- Some ripple lamination, showing a traction current
- Cross bedded sandstone within transition from pebbly sandstone into organic shale
- Organic shale at the top of fining upward
- Common mud draped and flaser indicating a tidal process. Some mud drape is associated with cross bedding.

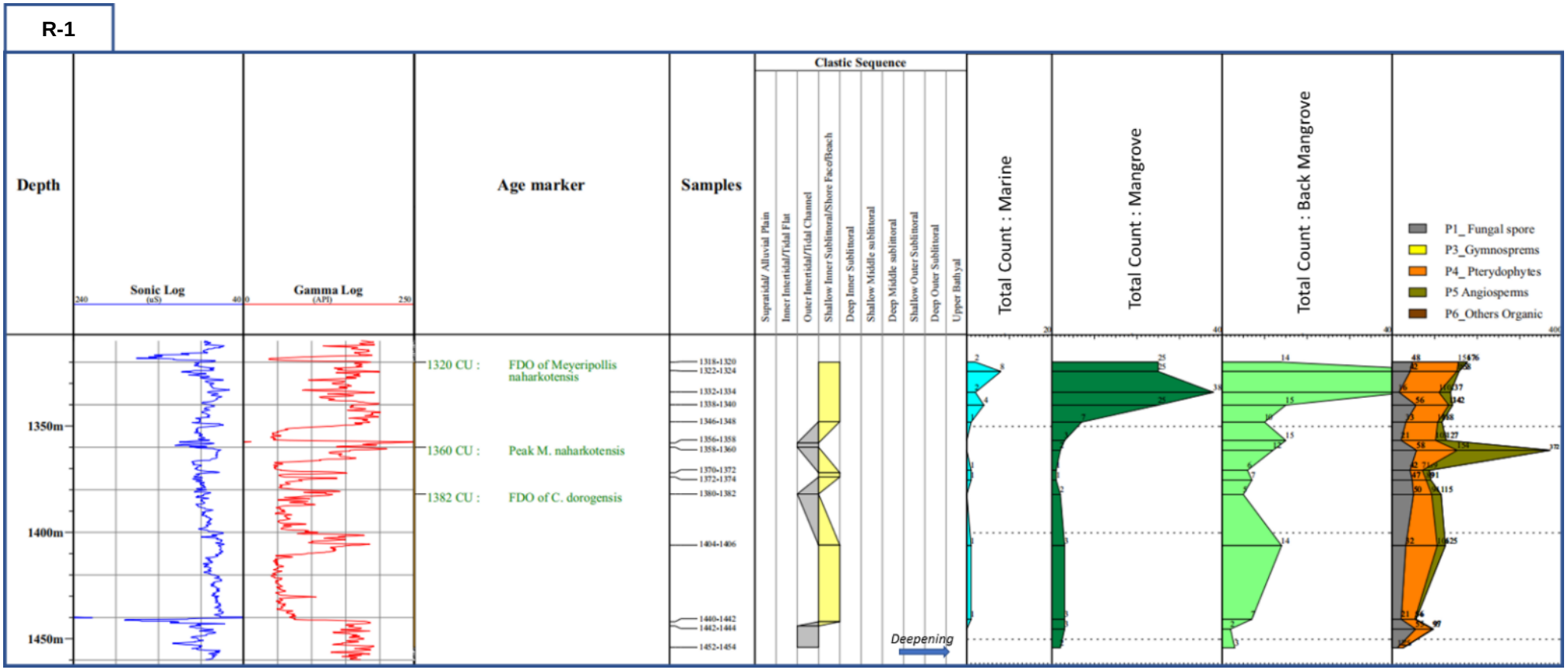


Figure 5: *Palynofacies analysis of R-1.*

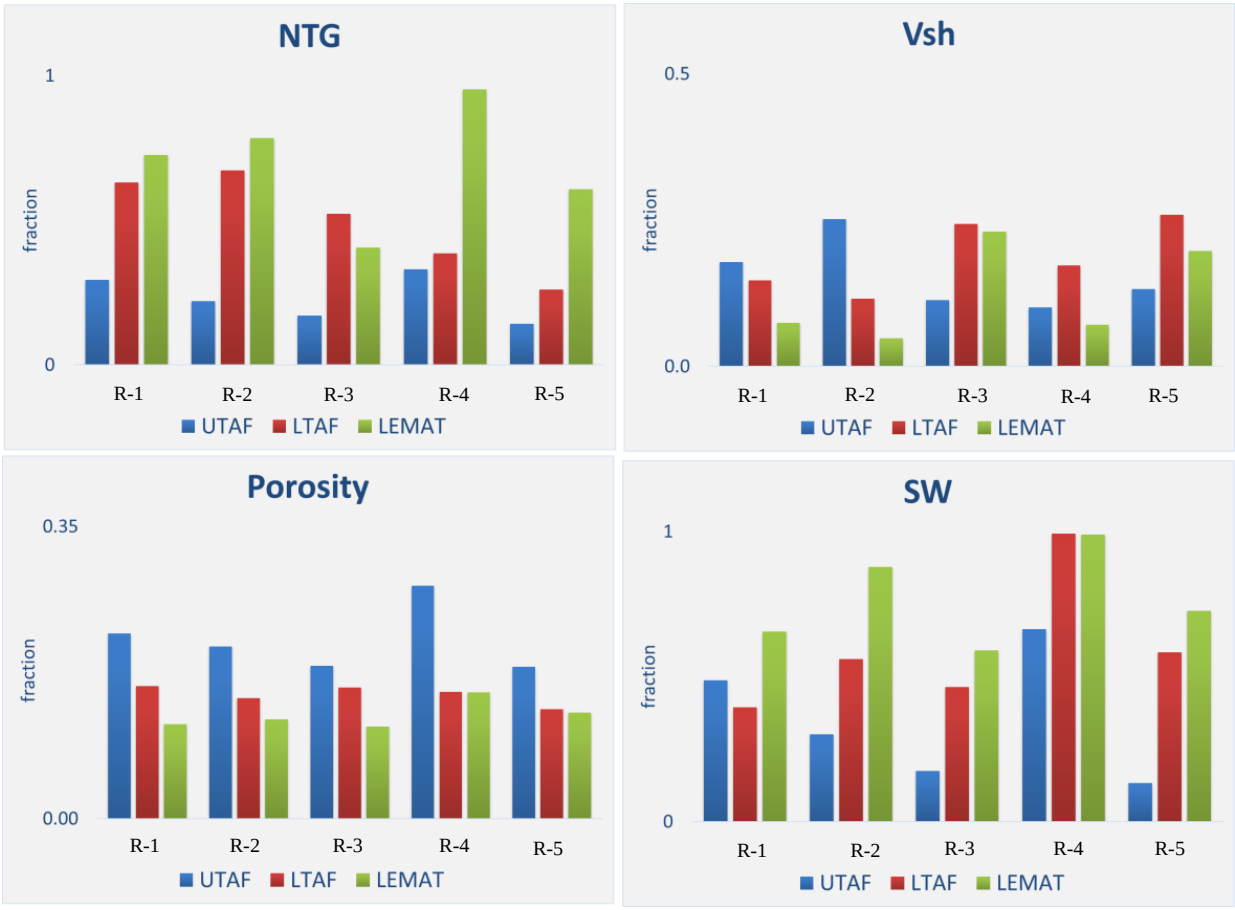


Figure 6: *Histogram shows the NTG, Vsh, Phie, and Sw of some wells in the Ridho field.*

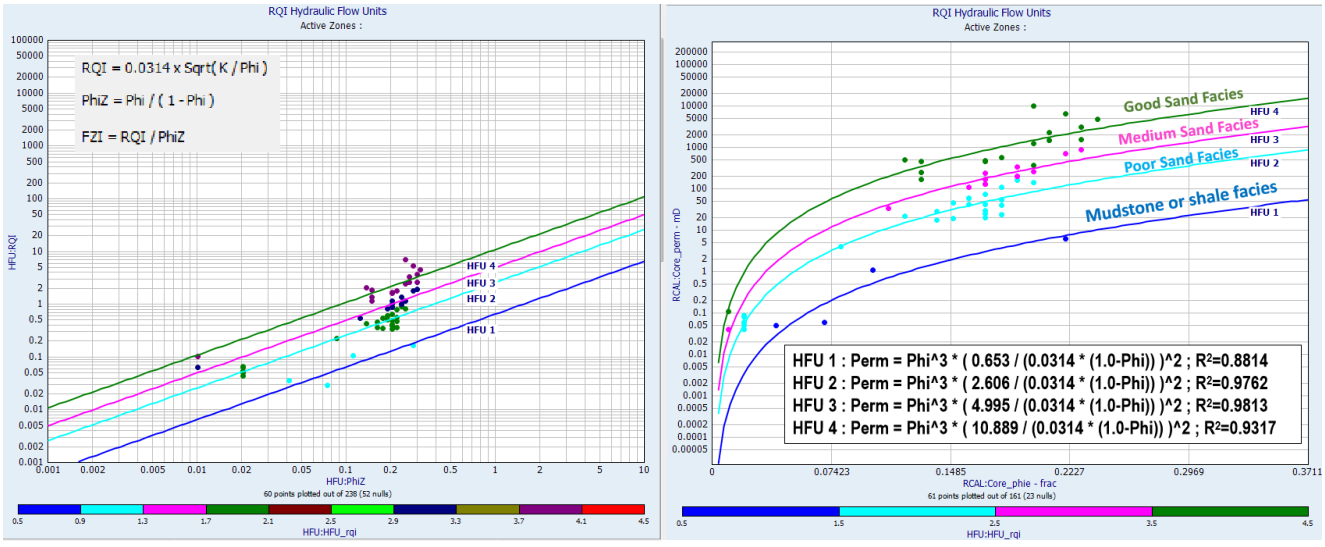


Figure 7: *(Left) The RQI vs PhiCore plot of R-2, R-3 and R-5. (Right) The HFU facies based on RQI methods.*

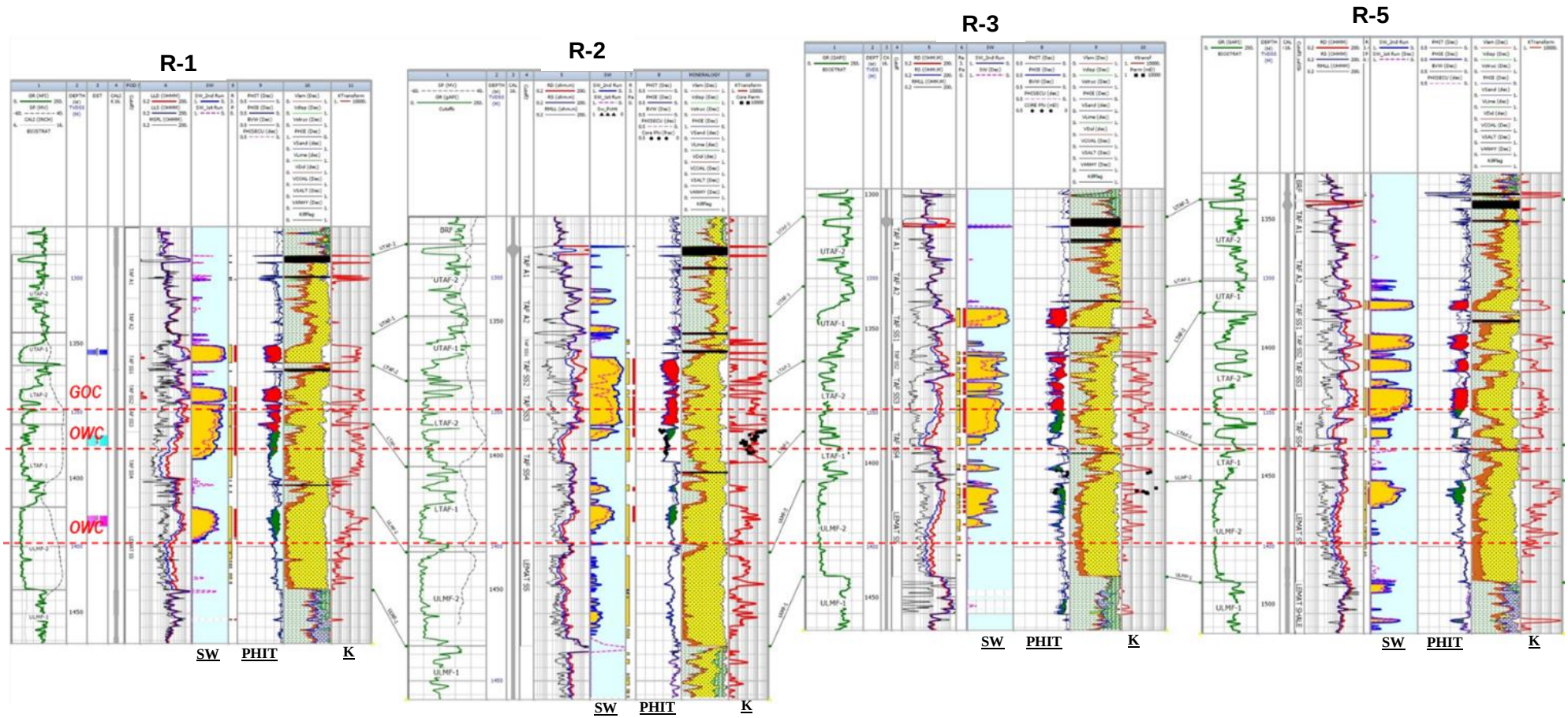


Figure 8: *Well section (flattened on TVDSS) of Ridho Field showing the result of petrophysical evaluation.*

The result from palynology analysis was also considered to interpret the depositional setting of Lower Talang Akar Formation. The palynology result is showing an intertidal with common back mangrove and higher plant spores. However, the mangrove and back-mangrove palynology signature is increasing to the Upper Talang Akar as the transgression occurred.

Common mud drape, flaser, lenticular sedimentary structures are showing traction current in tidal process. However, the depositional environment may not be too far from the source, as rock fragments are still remain. The Lower Talang Akar Formation is an early synrift sediment which common to have pebble of basement origin.

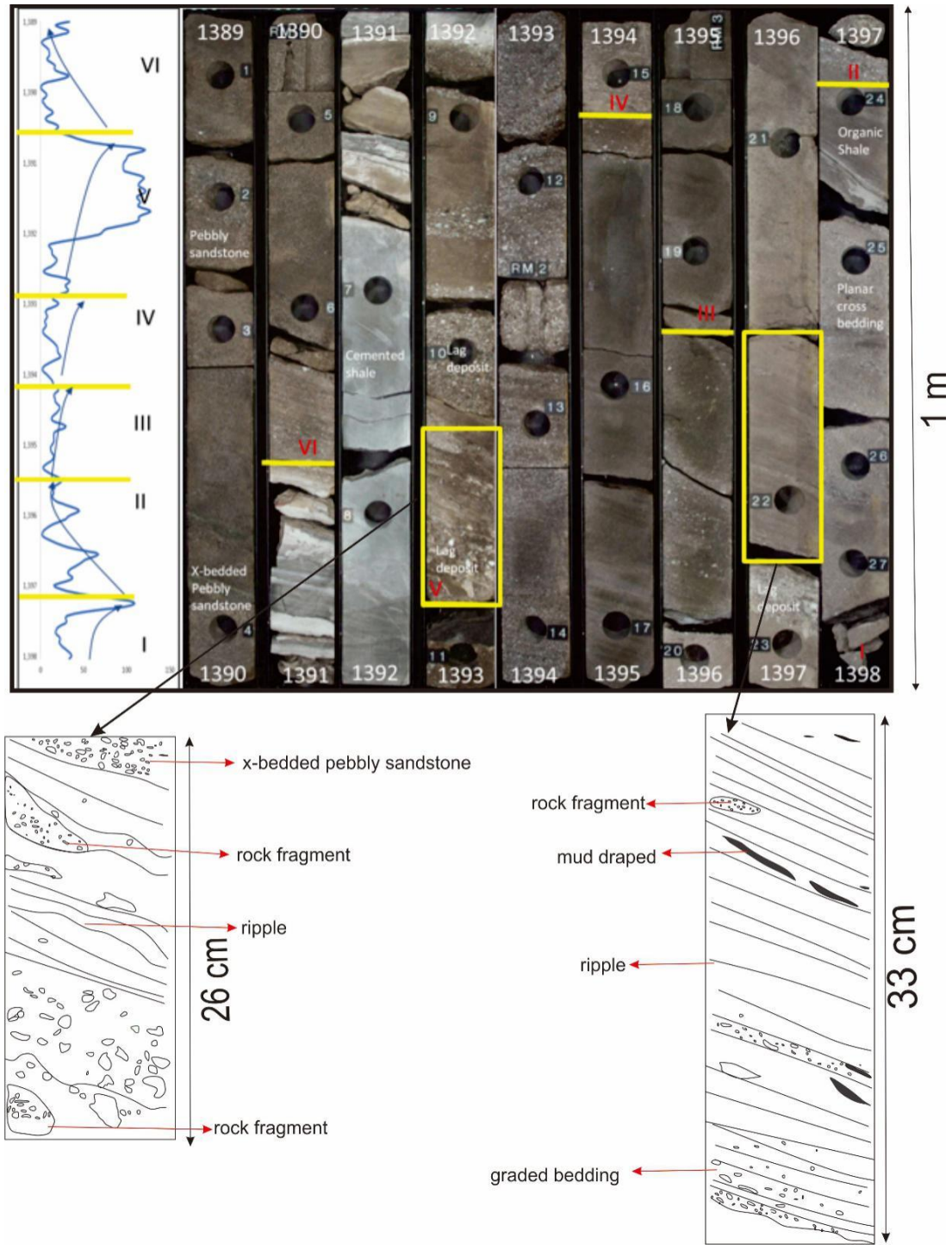


***Figure 9**: The core photograph along with core gamma with fining/coarsening upward signature of Lower Talang Akar Fm. The core gamma showing a good correlation to the grain size. The illustration below showing to emphasize of sedimentary structure in the core.*



Figure 10:

Typical of sandstone in the Upper Talang Akar Fm.

The core of Upper Talang Fm (left), is showing a cleaner sandstone with common cross bedding and mud drapes. As the marine transgression occurred, the sandstone become cleaner and rock fragment such as pebble become absent and the basement provenance is less prominent.

The reservoir geometry in this depositional environment is expected to be an isolated tidal channel which is perpendicular to the Oligocene shoreline.

DISCUSSION

A chronostratigraphy-driven well correlation was made for the Ridho Field, based on integration of data from wireline logs, petrophysical, palynology, sedimentology and special/routine core analyses. This integrated well correlation was not available when the field's POD was approved.

The palynology result is showing transgressive event from Lemat, Lower Talang Akar into the Upper Talang Akar Formation. The depositional environments changed from back-mangrove, mangrove, into shallow marine from Lemat, Lower Talang Akar, into Upper Talang Akar, respectively. As the transgression progressed, tidal influx become more persistent. This resulted in the development of isolated, sandy tidal channels within the upper part of Talang Akar, which should be perpendicular to Oligocene shoreline.

The transgression event created better reservoir quality due to the absence of mud and pebbles and better grain sorting within the Upper Talang Akar Formation. The better reservoir quality can be seen from core features, porosity-permeability data, and petrophysical analysis. The coarser grains associated with pebbles in the Lemat and Lower Talang Akar Formation indicate that their sediment source is relatively close, probably from exposed nearby basement. This was during a period of high energy fluvio-lacustrine depositional processes within the early synrift phase of North Palembang Sub-Basin development. However, the NTG of the Upper Talang Akar Formation is lower than Lower Talang Akar and Lemat Formation. This can be interpreted as the result of decreasing sediment supply and more distal environment that is also supported by a finer grains within the Upper Talang Akar Formation.

CONCLUSION

The chronostratigraphic sand units within Talang Akar and Lemat Formations in the Ridho Field were subdivided into: ULMF-2, LTAF-1, LTAF-2, UTAF-1, and UTAF-2. The depositional environments of Lemat and Lower Talang Akar Formation ranges from back-mangrove to mangrove, and then followed by shallow marine domination in the Upper Talang Akar Formation. The NTG in the Lemat and Lower Talang Akar is lower than it is in the Upper Talang Akar Formation. However, the reservoir property, such as Vsh, porosity, and permeability, are higher in the Upper Talang Akar than it is in the Lower Talang Akar and Lemat Formations.

REFERENCES

Barber, A.J., Crow, M.J., and Milsom, J.S. 2005. Sumatera: Geology, Resources and Tectonic Evolution. Geological Soeciety, London, Memoirs.

Bishop, M.G., 2001. South Sumatra Basin Province, Indonesia: The Lahat/Talang Akar-Cenozoic Total Petroleum System. USGS Open-file report 99-50S.

Cole, J. M., and Crittenden, S., 1997. Early Tertiary basin formation and the development of lacustrine and quasi-lacustrine/marine source rocks on the Sunda Shelf of SE Asia. In: Fraser, A. J., Matthews, S. J., and Murphy, R. W., eds., Petroleum Geology of Southeast Asia: Geological Society Special Publication No. 126, p. 147-183.

Courteney, S., Cockcroft, P., Lorentz, R., Miller, R., Ott, H.L., Prijosoesilo, P., Suhendan, A.R., Wight, A.W.R., 1990. South Sumatra. Indonesia - Oil

and Gas Fields Atlas, 3. Indonesian Petroleum Association, Jakarta, Indonesia.

De Coster, G. L. 1974. The geology of the Central and South Sumatra Basins. Proceedings of Indonesian Petroleum Association, 3rd Annual Convention, p. 77-110.

Hamilton, W., 1979. Tectonics of the Indonesian Region. Buletin Persatuan Geologi Malaysia (Bulletin Geological Society of Malaysia), 6, 1-345. Geological Society of Malaysia, Kuala Lumpur, Malaysia.

Longman, M.L., Siemers, C.T., Siwindono, T., 1992. Characteristics of low-relief carbonate mudbank reservoir rocks, Batu Raja Formation (Lower Miocene), Air Serdang and Mandala fields, South Sumatra Basin, Indonesia. In: Siemers, C.T., Longman, M.W., Park, R.K., Kaldi, J.G. (ed), Carbonate Rocks and Reservoirs of Indonesia: a Core Workshop, Indonesian Petroleum Association Core Workshop Notes, 1 (9).

Nichols, G. (2009). Sedimentology and stratigraphy (2nd ed.). Chichester, UK ; Hoboken, NJ: Wiley-Blackwell

Netherwood, R. 2000. The petroleum geology of Indonesia, overview of Indonesia's oil and gas industry. In: Indonesia 2000 Reservoir Optimization Conference, Jakarta, PT. Schlumberger Indonesia, p. 174-227.

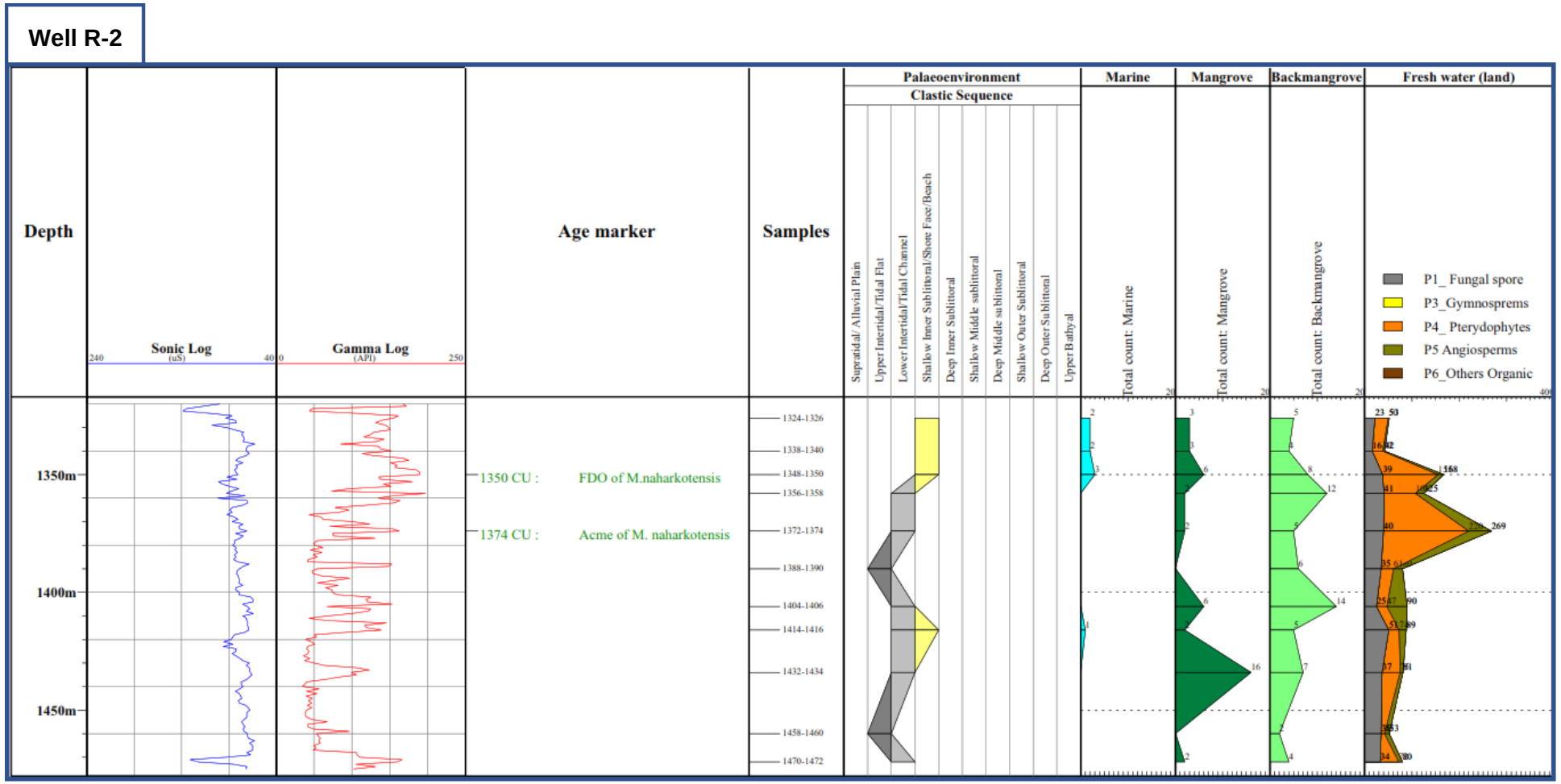
Situmeang, S.P., Zeliff, C.W., Lorentz, R.A., 1992. Characterisation of low relief carbonate banks, Baturaja Formation, Ramba A and B pools, South Sumatra, Indonesia. In: Siemers, C.T., Longman, M.W., Park, R.K., Kaldi, J.G. (ed), Carbonate Rocks and Reservoirs of Indonesia: a Core Workshop, Indonesian Petroleum Association Core Workshop Notes, 1 (8).

Suhendan, A. R., 1984. Middle Neogene depositional environments in Rambutan area, South Sumatra. Proceedings of Indonesian Petroleum Association, Thirteenth Annual Convention, May, 1984, p. 63-73.

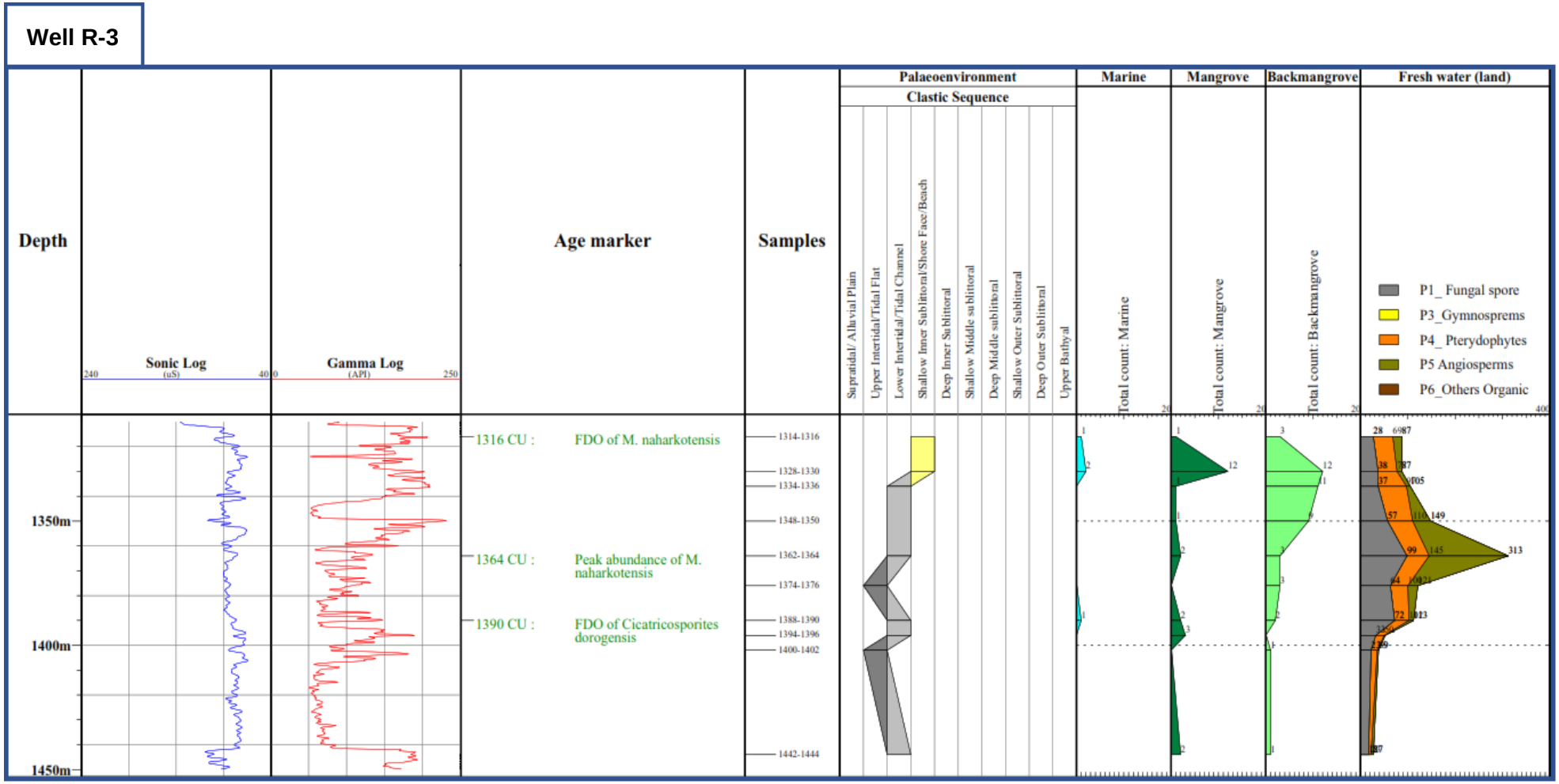
Syaifudin,M., Subroto, E.A., Noeradi,D., Kesumajana, A.H.P., 2015. Characterization and correlation study of source rocks and oils in Kuang area, South Sumatra basin: the potential of Lemat formation as hydrocarbon source rocks, Proceedings Indonesian Petroleum Association, Thirty-Ninth Annual Convention and Exhibition, Jakarta, Indonesia.

van der Zwan CJ. 1990. Palynostratigraphy and palynofacies reconstruction of the Upper Jurassic to Lowermost Cretaceous of the Draugen Field, offshore mid Norway. Rev Palaeobot Palyno. 62:157-186.

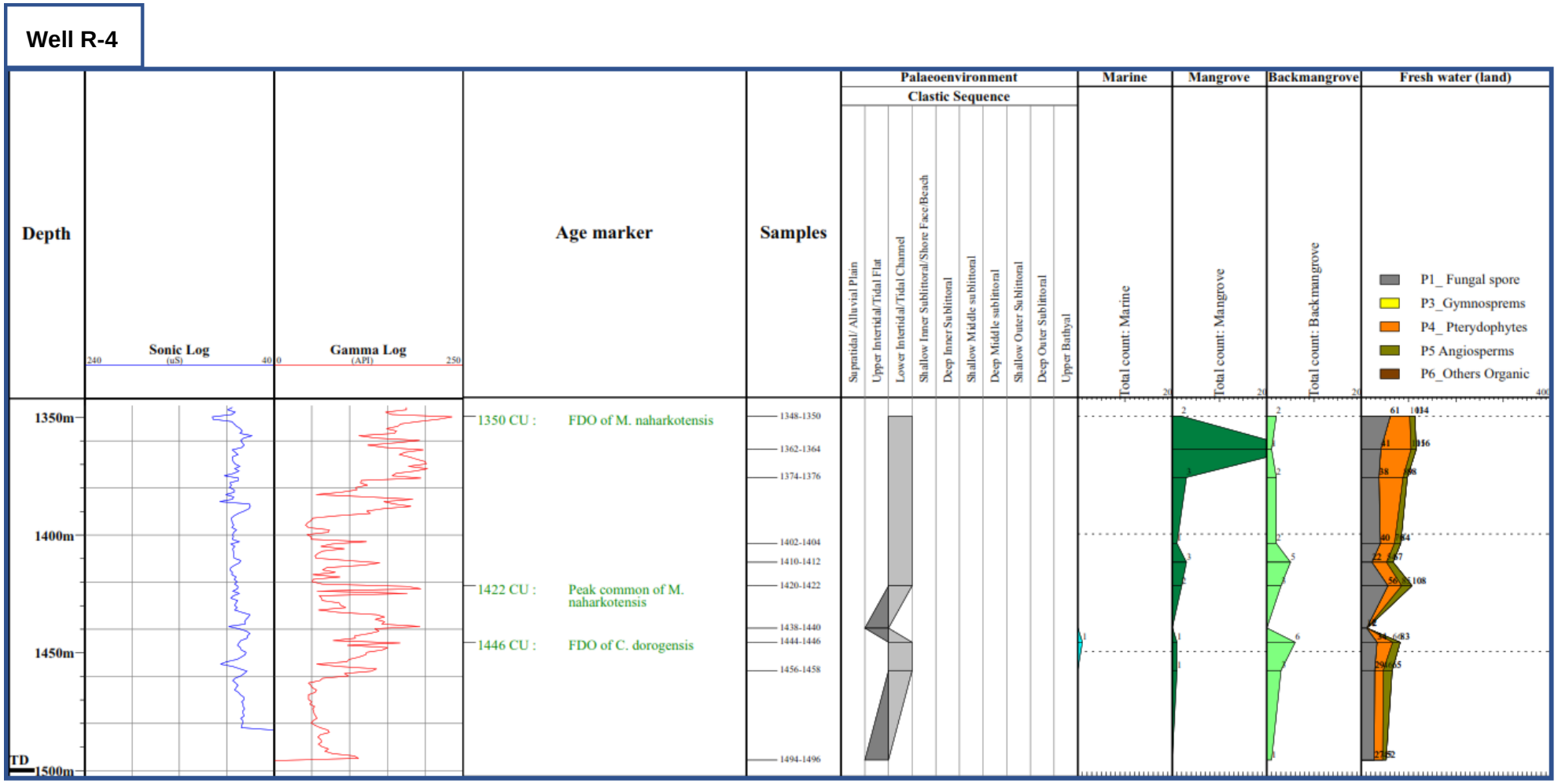
Whitaker MF, Giles MR, Cannon JC. 1992. Palynological review of the Brent Group, UK sector, North Sea. In: Morton AC, Haszeldine RS, Giles MR, Brown S, editors. Geology of the Brent Group. Geological Society of America Special Publications 61; p. 169-202.



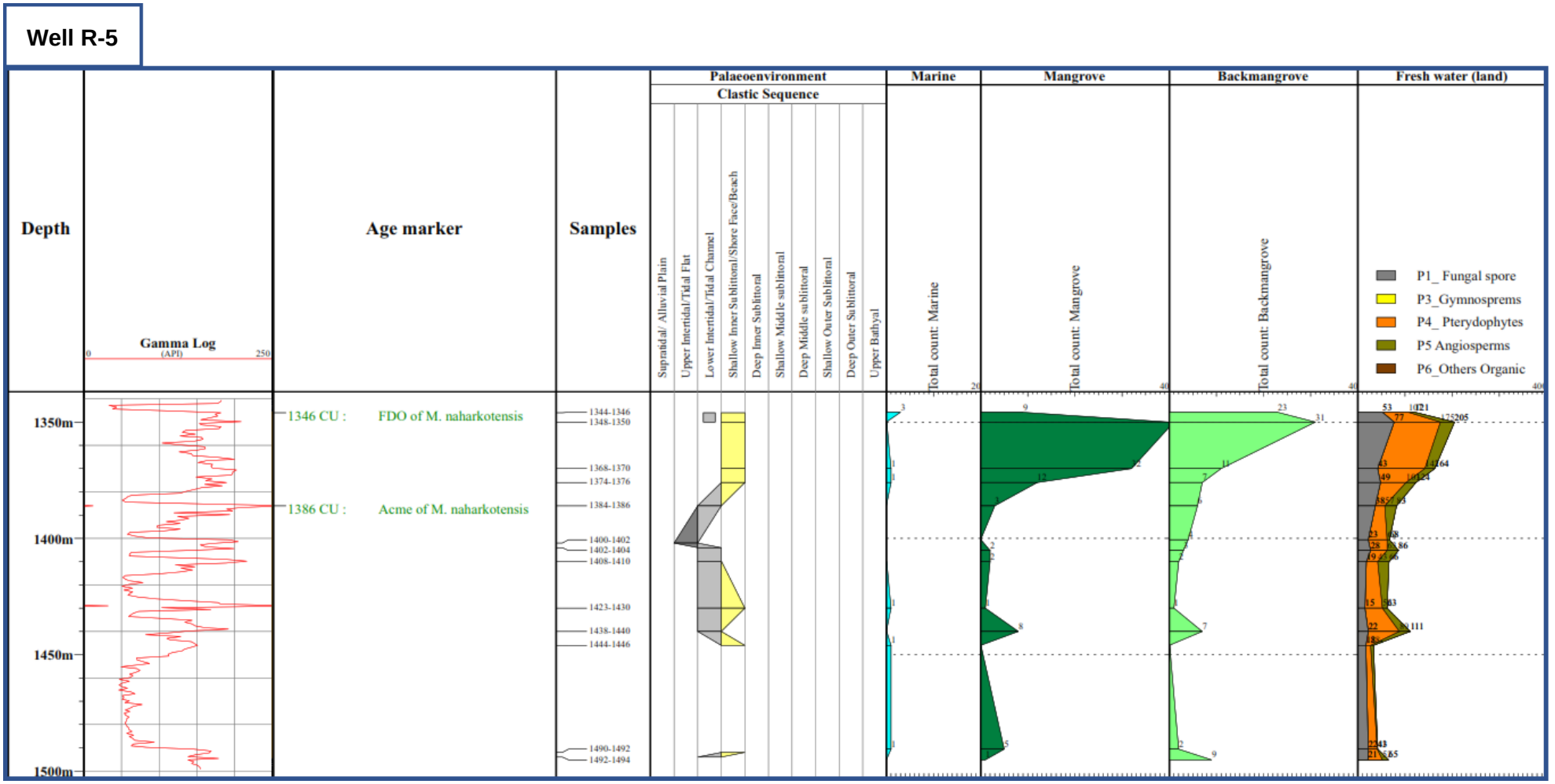
Appendix 1. *Palynofacies analysis of R-2*



Appendix 2. *Palynofacies analysis of R-3*



Appendix 3. *Palynofacies analysis of R-4*



Appendix 4. *Palynofacies analysis of R-5*

Sedimentary Basins of Indonesia: Outline and Thickness Variation Understanding

Herman Darman[*] and Doddy Yuliong B.A.

Indogeo Social Enterprise
[*]Currently with PETRONAS Sdn. Bhd. Kuala Lumpur, Malaysia

INTRODUCTION

Offshore petroleum exploration in Indonesia began in late 1960's and thereafter a significant number of seismic data sets were acquired. Based on these data, several basin outline maps were generated such as those published by Hamilton (1974), BEICIP FRANLAP (1992), and Sujanto (1997). Based on these data sets, 60 sedimentary basins were officially recognized by the Government of Indonesia (Sunarjanto et al., 2007 included in 2008 publication). The outlines of the basins were used as a reference by government officials and the petroleum industry. Recently, the Geological Agency published a map which shows 128 sedimentary basin outlines in Indonesia. Unfortunately, these maps were not accompanied with supporting subsurface data.

The understanding of those sedimentary basins is very important for petroleum exploration, as they are basically the places to find hydrocarbons. Petroleum potential within a basin is related to its sediment accumulation and tectonic history. Critical petroleum system elements such as source rocks, reservoir and seal mainly comprise sedimentary rocks. The order of deposition, quantity of sediments and basin history will control the effectiveness and quantity of hydrocarbon generation in a particular basin.

This article will go through the history of various basin outline maps and aim to provide additional information, such as basement depth, to give further detail on the basins in Indonesia. There are some detailed maps which show the distribution of oil and gas fields, which are obviously related to sediment thickness.

BASIN STATUS AND DISTRIBUTION

Several basin outline maps have been published and the authors have classified the status of the basins into: basin with production, basin with hydrocarbon discovery, basin with exploration wells but no discovery and undrilled basins (e.g. Sujanto, 1997 and Netherwood, 2000). The latter add a statistical comparison of basin distribution between the west and east of Indonesia (Figure 1). Several authors came with the same classification but different number of basins. The numbers of producing basins have increased as more exploration successes brought the hydrocarbon on stream. The numbers of undrilled basins are also increased within Indonesia territory. BPMIGAS/LAPI-ITB (2008, in Satyana, 2011), almost double the number of undrilled basins compared to Sunarjanto et al. (2008), which was published only a year before. The number of total sedimentary basins according to the Geological Agency (2009) also increased by 50% compared to the BPMIGAS/LAPI-ITB version (Figure 2).

The significant changes on the number of basins like the total and undrilled basins probably require a detailed look. The basins' definition and boundary are key support to these numbers. The data and reason for classification behind the number of basins were incomplete in these publications.

Sunarjanto et al. (2008) applied GIS (Geographic Information System) in the study and referred to sedimentary thickness map, gravity anomaly and age analysis in defining the basin outlines (Figure 3). The known comprehensive sediment thickness map available at that time was a map which was published by Hardy et al. (1997) [Figure 4] as a result of collaboration between Pertamina and Unocal. At the time, probably Pertamina had the most comprehensive subsurface data in Indonesia. Although the map was rough, it provided good understanding of the depth of each key basins in Indonesia.

The Geological Agency generated a map with the largest number of basins in 2010 (Figure 5). This map defined 128 basins and included shallow and young basins which are most likely non-prolific for hydrocarbons. BPMIGAS and LAPI-ITB generated a map with the second largest number of basins (86 basins, Figure 6), where Pre-Tertiary (Mesozoic and older) basins were separated from the Tertiary (Cenozoic) basins. Based on the outlines, this map includes young sedimentary basins and splits the outline of previously defined basins. The sediment thickness map, like Hardy et al. (1997), should be updated and used as a basis of the basin definition.



Western Indonesia

NSB - North Sumatra
CSB - Central Sumatra
SSB - South Sumatra
NSF - North Sumatra fore arc
SSF - South Sumatra fore arc/Bengkulu
S/A - Sunda/Asri
NWJ - Northwest Java
JF - Java fore arc
EJ - East Java/Java Sea
BI - Billitong
PE - Pembuang
BA - Barito
PN - Pater Noster platform
AA/P - Asem-Asem/Pasir
UK - Upper Kutei
K/MS - Kutei/Makassar Straits
MU - Muara
TA - Tarakan
CE - Celebes
KE - Ketungau
ME - Melawai
WN - West Natuna
EN - East Natuna

Eastern Indonesia

SM/NM - South/North Minahasa
GO - Gorontalo
B/S - Banggai–Sula
S/M - Salabangka–Manui
BU - Buton
BD - Banda
B - Bone
F - Flores
SS - Spermonde/Selayar
L - Lariang
SBL - South Bali–Lombok
SA - Savu
TI - Timor
NWSZOC - Northwest Shelf zone of cooperation
W - Weber
SE - Seram
NEH - Northeast Halmahera
EH - East Halmahera
SEH - Southeast Halmahera
SW - Salawati
BT - Bintuni
MO - Misool-Onin
TBA - Teluk Berau–Ajumaru
KT - Kai Tanimbar
A - Aru
AK - Akmeugah
AR - Arafura
CIJ - Central Irian Jaya
W/W - Waipoga/Waropen

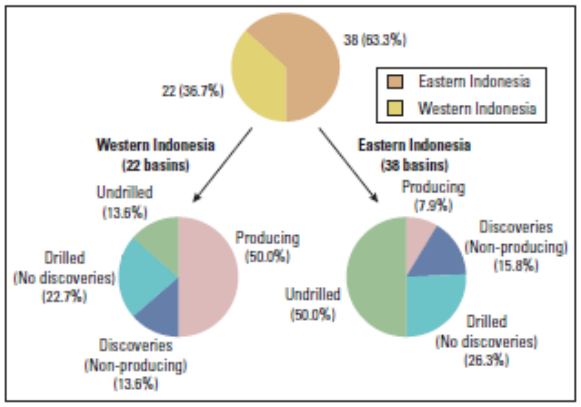


Figure 1: *Indonesian basin classification and their exploration status after Sujanto, 1997; Sumantri and Sjahbuddin, 1994 (Netherwood, 2000).*

Year	Author / Institute	Producing Basin	With discovery	Without discovery	Undrilled basin	Total basins
1997	Sujanto	14	10	14	22	60
2000	Netherwood, R. / Schlumberger	14	10	14	22	60
2007	Avicenia et al. / BPMIGAS	15	9	14	22	60
2007	Sunarjanto et al. / LEMIGAS	16	8	15	24	63
2008	BPMIGAS / LAPI-ITB	17	11	16	42	86
2009	Geological Agency	----unclassified ----				128

Figure 2: *Number of Indonesian sedimentary basins and their classification according to several authors.*

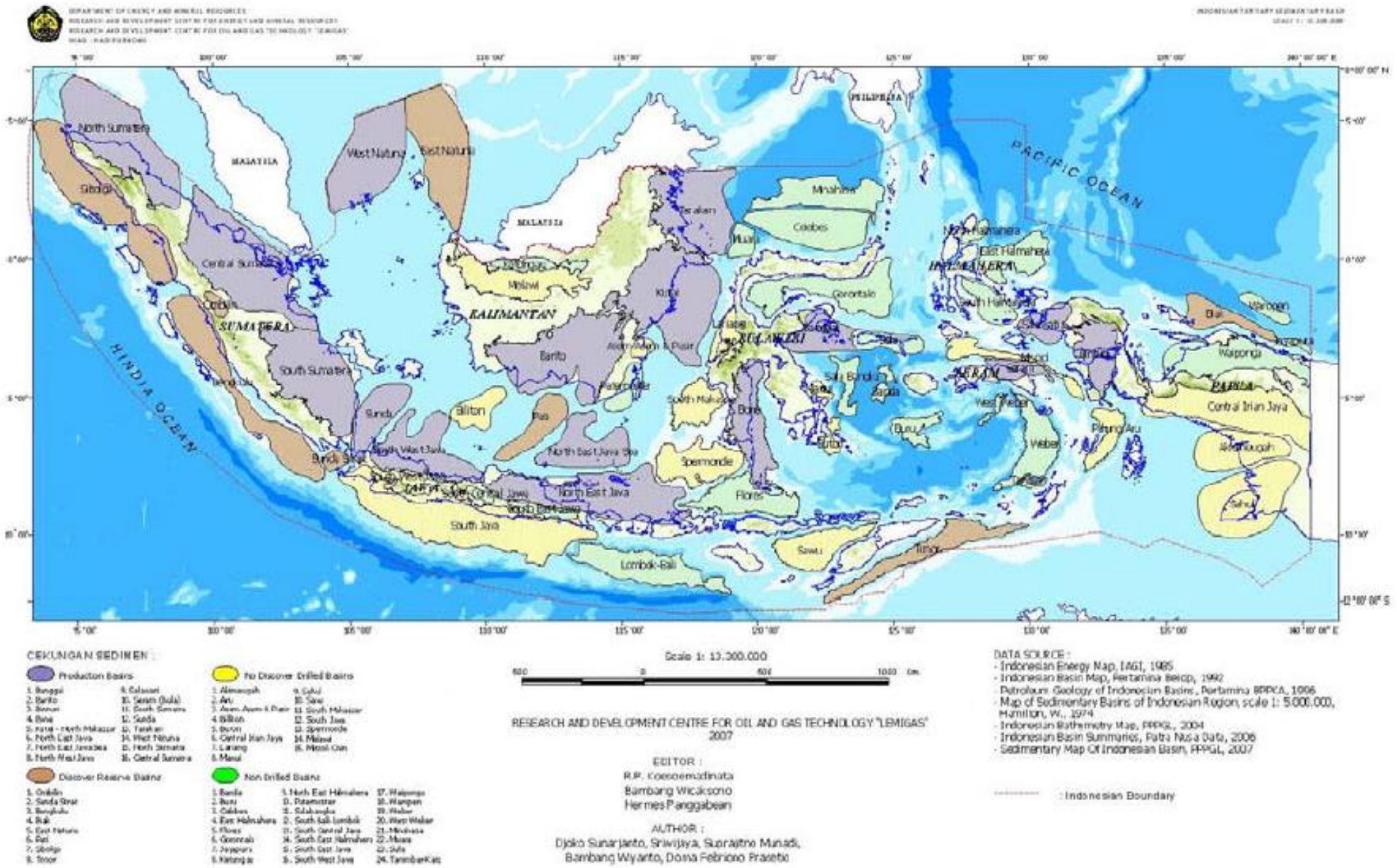


Figure 3: *Indonesian sedimentary basin outlines published by Sunarjanto et al., from LEMIGAS, in 2007, published in 2008, with total of 63 basins.*

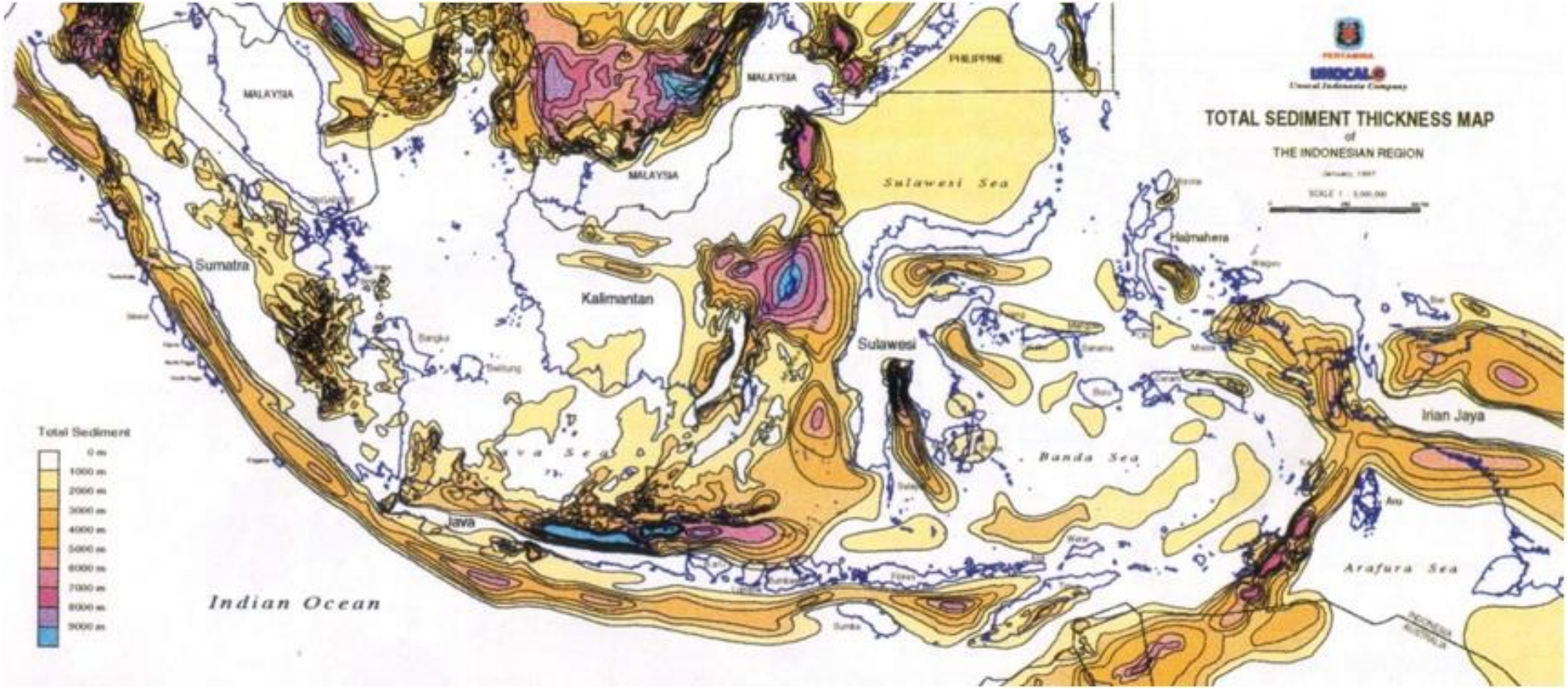


Figure 4: *Total sediment thickness map of Indonesia by Hardy et al. (1997).*

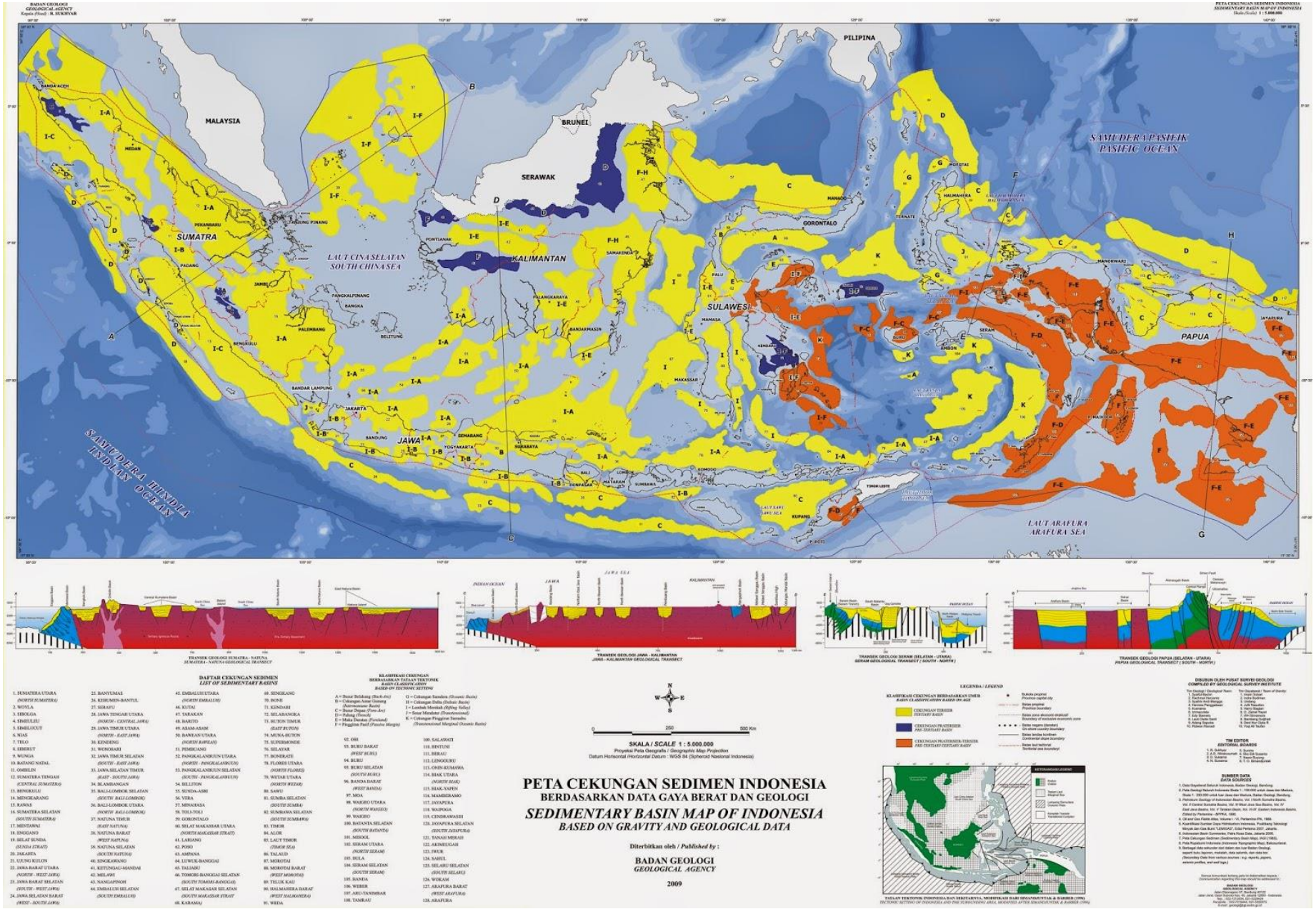


Figure 5: *Indonesian basin outlines according to the Geological Agency (2009). There are 128 sedimentary basins identified including Tertiary, pre-Tertiary and a combination of Tertiary and pre-Tertiary basins.*



Figure 6: *Indonesian basin outlines published by BPMIGAS and LAPI-ITB (2008), showing the distribution of 86 sedimentary basins in Indonesia.*

INDIVIDUAL BASIN WORK

Continuous acquisition of subsurface data in various basins provides better understanding of how deep and how thick sediment fill of the basins are. The lateral distribution of the sediments is also better defined. The best basin definitions are usually provided by operating companies in the corresponding basins. Some companies are also using gravity data as seismic data may not define the deeper part of the basins. The operators do detailed work using the available data, as they aimed to understand the basins in great detail for exploration. Several examples of sediment thickness or depth to basement maps are discussed in the following sections.

The North Sumatra Basin is the westernmost producing basin in Indonesia. The basin's depth to basement map (Figure 7) shows basements high in the southeast and the deeper part of the basin is located in the north, in the areas called Jawa Deep and Lhok Sukon Deep (after Anderson, 1993). Both depocenters are deeper than 5 seconds TWT (two way time), which could be up to 8 kilometers thick of sediments below the sea bottom. The north –south horst and graben trends are typical for this basin. The largest field is Arun Gas field, located on the Arun High which separates those two deeps or depocenters. The horst and graben in the eastern part of the basin are well defined on the seismic data. The majority of onshore oil fields are located in the southeast of the area, resulted from early exploration in Indonesia back in 1800s era. The first commercial oil discovery well, Telaga Tunggal-1, was drilled in this area.

In the Central Sumatra Basin, the depth to basement contours and faults show NW-SE and N-S trend (Figure 8). The N-S trend is considered the older structural element and it continues northwards to the Malaysian Peninsula. A large depocenter is located in the northwest of Duri, Minas and Kotabatak fields, and the sediments here are thicker than 2000 meters. Sediment thickness in the basin is thinning northward. The NW-SE trend of Barisan Mountain and/or Great Sumatra Fault system bounded the southern part of the basin. Figure 8 is a modified version after Heidrick & Aulia (1993) and Barber and Crow (2005). Oil and gas field outlines were added to the map to show their relative position to the basement deep and their orientation related to the fault trends.

Figure 9 shows the depth to basement map of the South Sumatra Basin with Central Palembang Basin right at the center of the basin (after Barber & Crow, 2005; and Ginger & Yielding, 2005). The depocenters are deeper than 4 seconds TWT or up to 6 to 7 kilometers thick of sediments below the surface. The larger fields are located around the depocenter. A number of fields were also discovered around the Muara Enim Deep. Barisan Mountains in the south is dominated by Quaternary volcanic deposits. The sediment thickness is much less towards the north of Malacca Strait.

The depocenter of the North West Java Basin is located in the south (Noble et al., 1997; Figure 10), which is thicker than 3 seconds TWT below the surface or approximately around 4 kilometers thick of sediments. In general, hydrocarbons in the basin migrate northward from the depocenter in the south. The basin is getting shallower towards Sunda Platform in the north. Isolated depocenters are identified in the northwest of the Northwest Java Basin, namely Sunda and Asri Basins. These basins are separated from the NW Java Basin by the Seribu Platform. A mix of oil and gas are found in this basin, but gas is more dominant.

Similar to the Northwest Java Basin, the East Java Basin has the depocenter located in the south (Nawawi et al., 1996 and Kenyon, 1977), which is deeper than 2 second TWT, approximately more than 3 km thick. The W–E structural trend in the south (Figure 11) are dominated by an inverted wrench fault zone, which is exposed well in the Madura Island. This structural trend extends westwards to onshore Java Island and eastwards to the Kangean Island. Towards the north there are troughs and arches which have SW-NE trend, following the paleo-subduction zone.

SEDIMENT THICKNESS MAPS UPDATE

Basinal sediment thickness or depth to basement maps are available for most of the producing basins, especially in the basin center area. To the basin margin where less hydrocarbon is expected, there will be less seismic and well data to create such maps. In the basin margin and also inter-basinal areas, outcrop and gravity data are useful for joining the depth to basement maps. Outcropping basement give a good control for such maps.

Integration of several depth to basement maps from different basins in Southeast Asia is shown in Figure 12. Apart from using existing published maps, there are others unpublished information which are integrated into this map. On top of that, well tops, gravity anomaly and outcrop data were also used to control the distribution of the contours.

The outcropping basements are colored in dark green. The outline of these outcrops indicated the 0 contour line of the sediment thickness map. The Malay Basin in Malaysia is the deepest basin in the region, followed by the Kutei Basin in East Kalimantan. Northwest Borneo Basin is the largest basin in the region. Thick sediment accumulation are identified in the southern part of the Celebes Sea, but they are relatively young (e.g. Pliocene – Pleistocene dominated sediments). Unfortunately, this area has almost no well control, and these contours are purely based on gravity map interpretation.

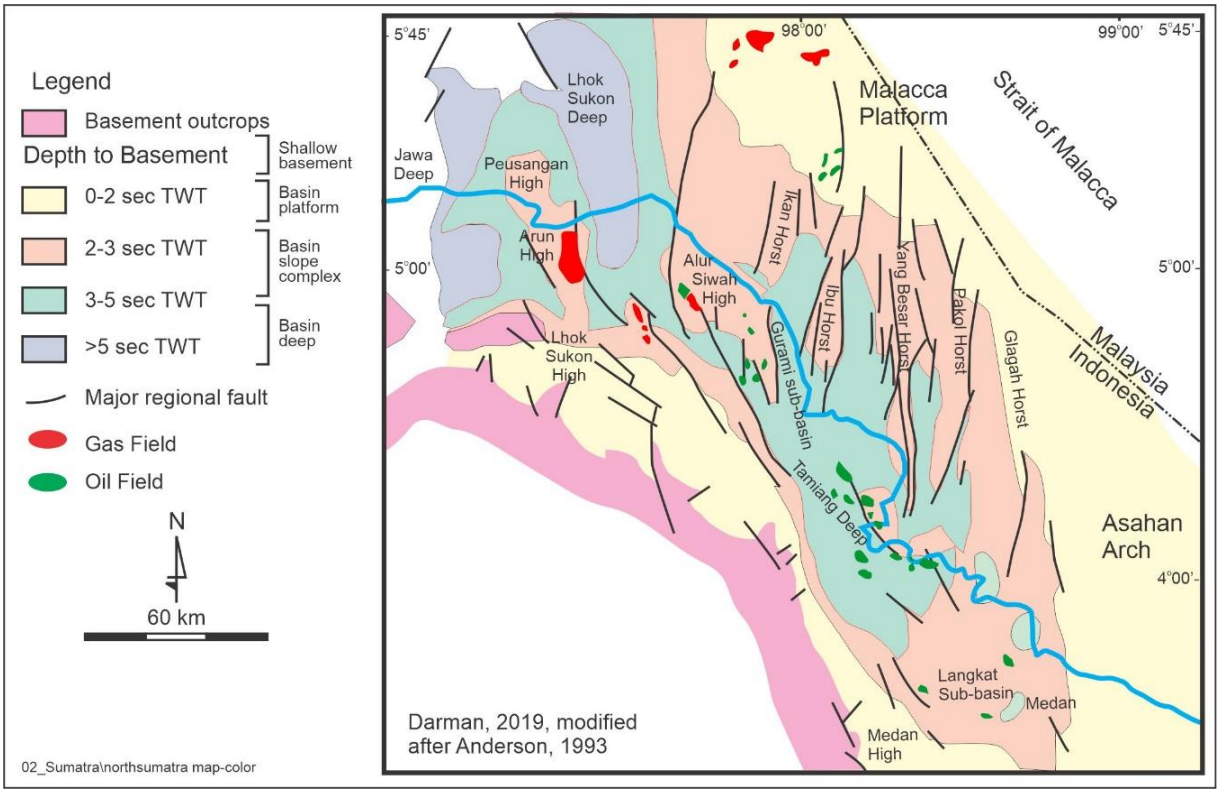


Figure 7: *Depth to basement map of North Sumatra Basin shows the isochrone contours in Two-Way-Time. The map shows the position of oil and gas fields relative to the depocenters.*

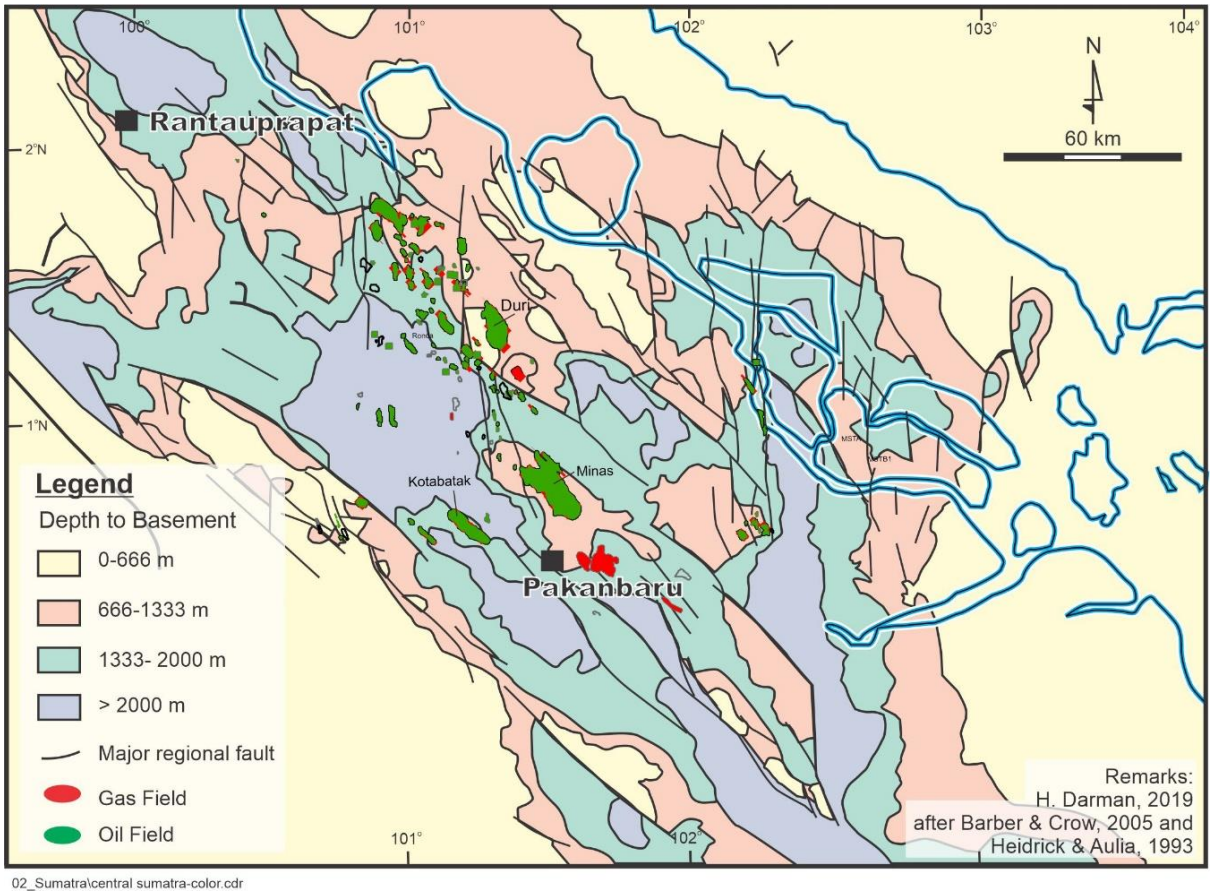


Figure 8: *Depth to basement map of Central Sumatra Basin shows the isochore contours in meters. The map shows the position of oil and gas fields relative to the depocenters.*

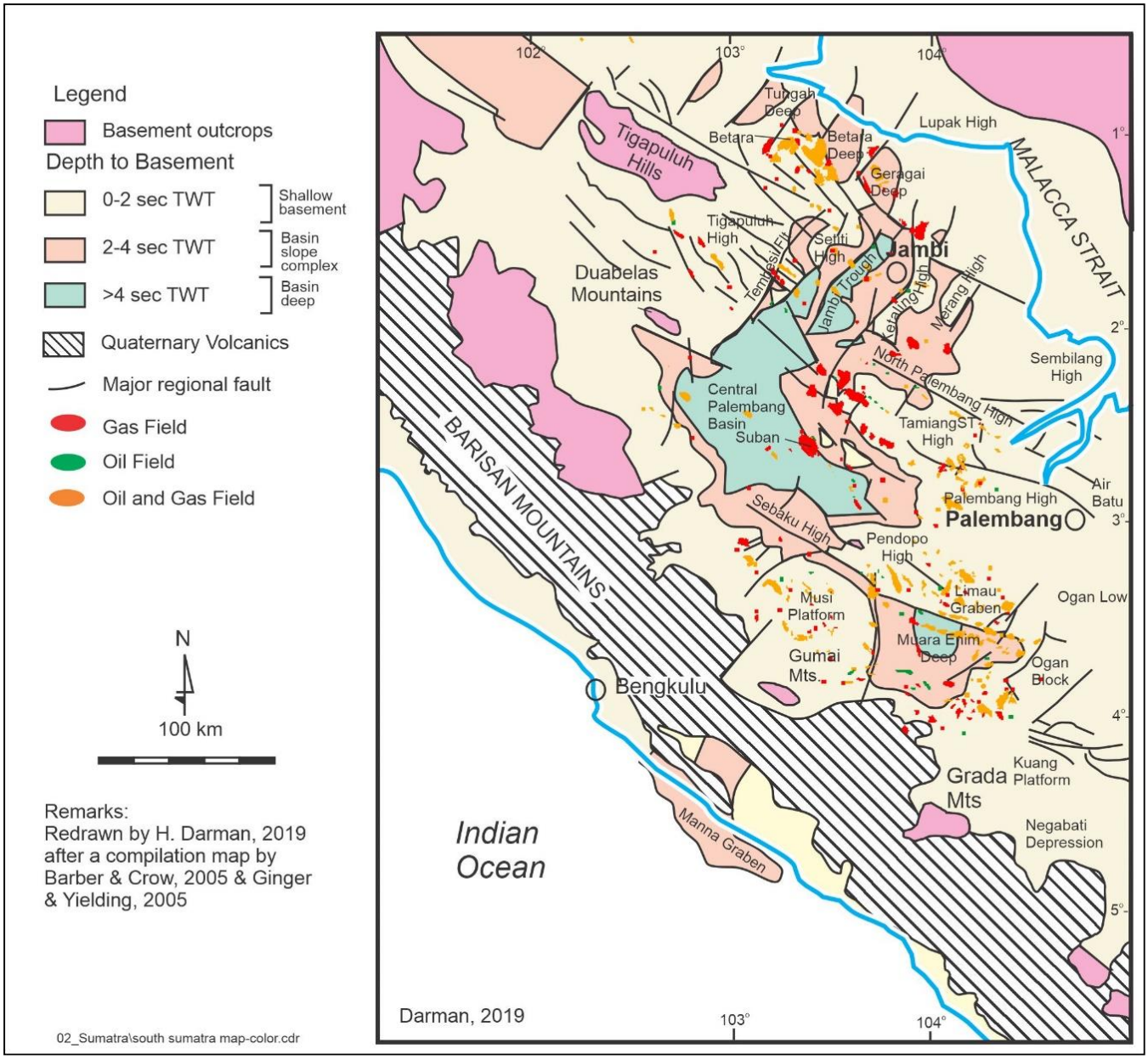


Figure 9: *Depth to basement map of South Sumatra Basin shows the isochrone contours in Two-Way-Time. The map shows the position of oil and gas fields relative to the depocenters.*

Apart from the Salawati Basin in the Bird Head of Papua, the sediment thickness contours in Eastern Indonesia basins generally have poor well control. The basement outcrop data from Buru, Seram, Timor, Halmahera and Papua provide a degree of confident on the understanding of basinal extend.

DISCUSSION

The sediment thickness map generated by Indogeo Social Enterprise (Figure 12) map is available in GIS version and will be revisited after a certain period of time or when new data are available. In the GIS, the map can be easily overlain by concession outlines and the companies that have better data can easily correct the map. More detailed gravity modelling may also help to improve the sediment thickness map.

Apart from potential map refinement by using new data, the map is also expected to be a tool to facilitate discussions between different operators in the same basins or for general discussion related to geosciences. The contours in this map will give additional data on top of the gravity data which is available online, such as those from Scripps Institution of Oceanography, University of California San Diego, USA (topex.ucsd.edu). As geoscientists, overlying maps onto the sediment thickness map would be a key to quickly determine which basins are potentially prolific for hydrocarbons, but perhaps little exploration activities were done so far therefore further study is necessary.

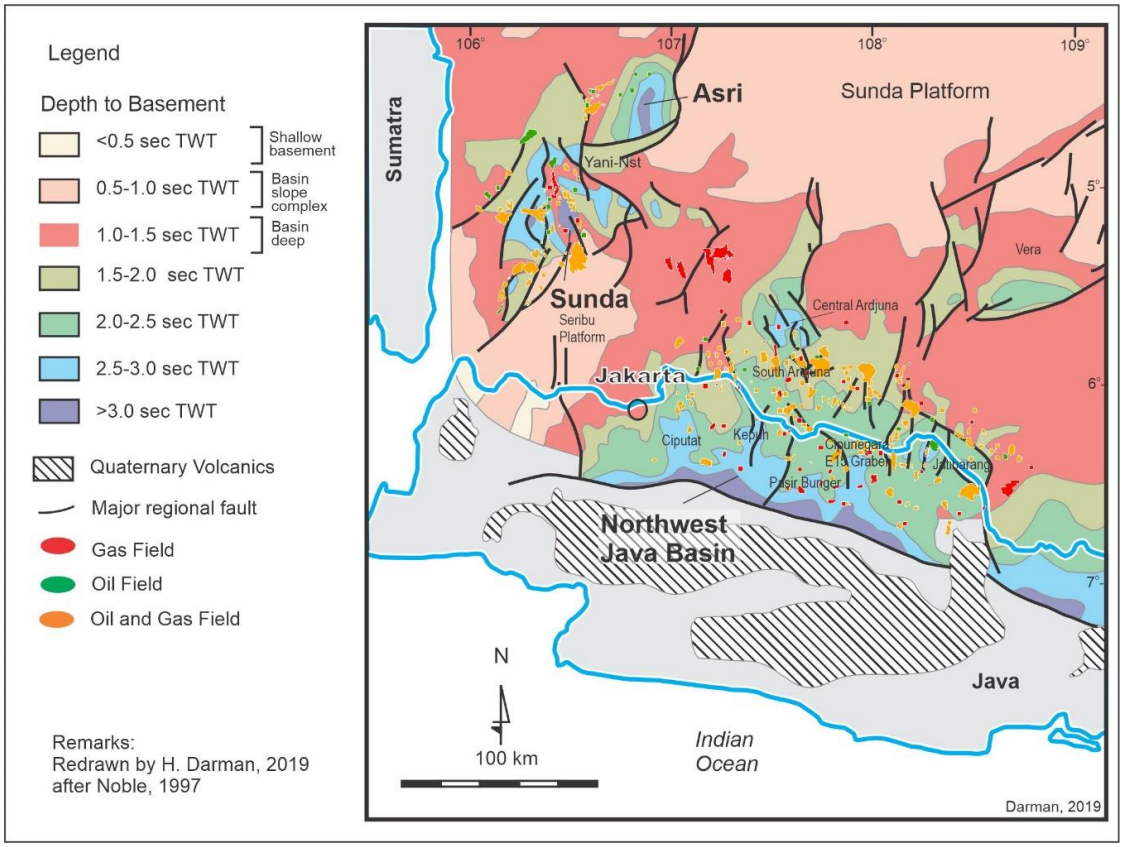


Figure 10: *Depth to basement map of Northwest Java Basin shows the isochrone contours in Two-Way-Time. The map shows the position of oil and gas fields relative to the depocenters.*

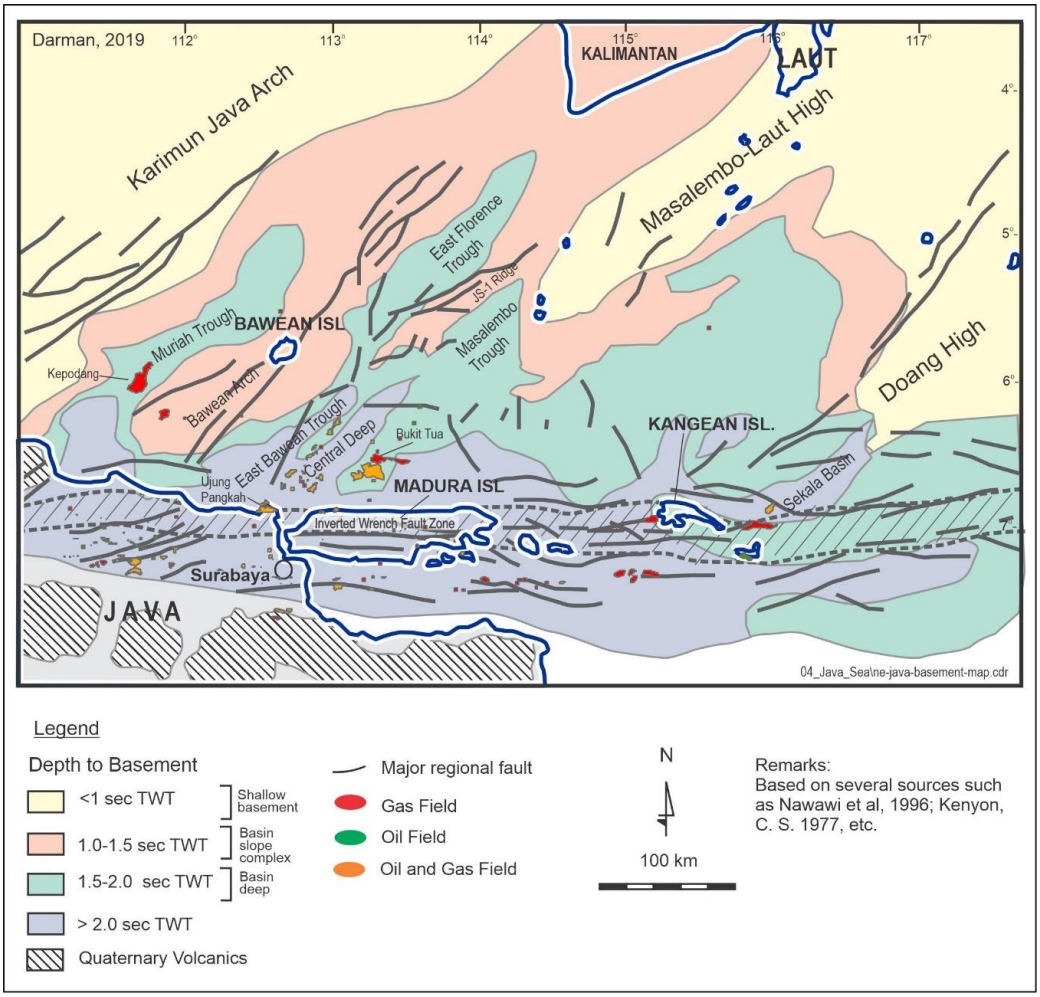


Figure 11: *Depth to basement map of East Java Basin shows the isochrone contours in Two-Way-Time. The map shows the position of oil and gas fields relative to the depocenters.*

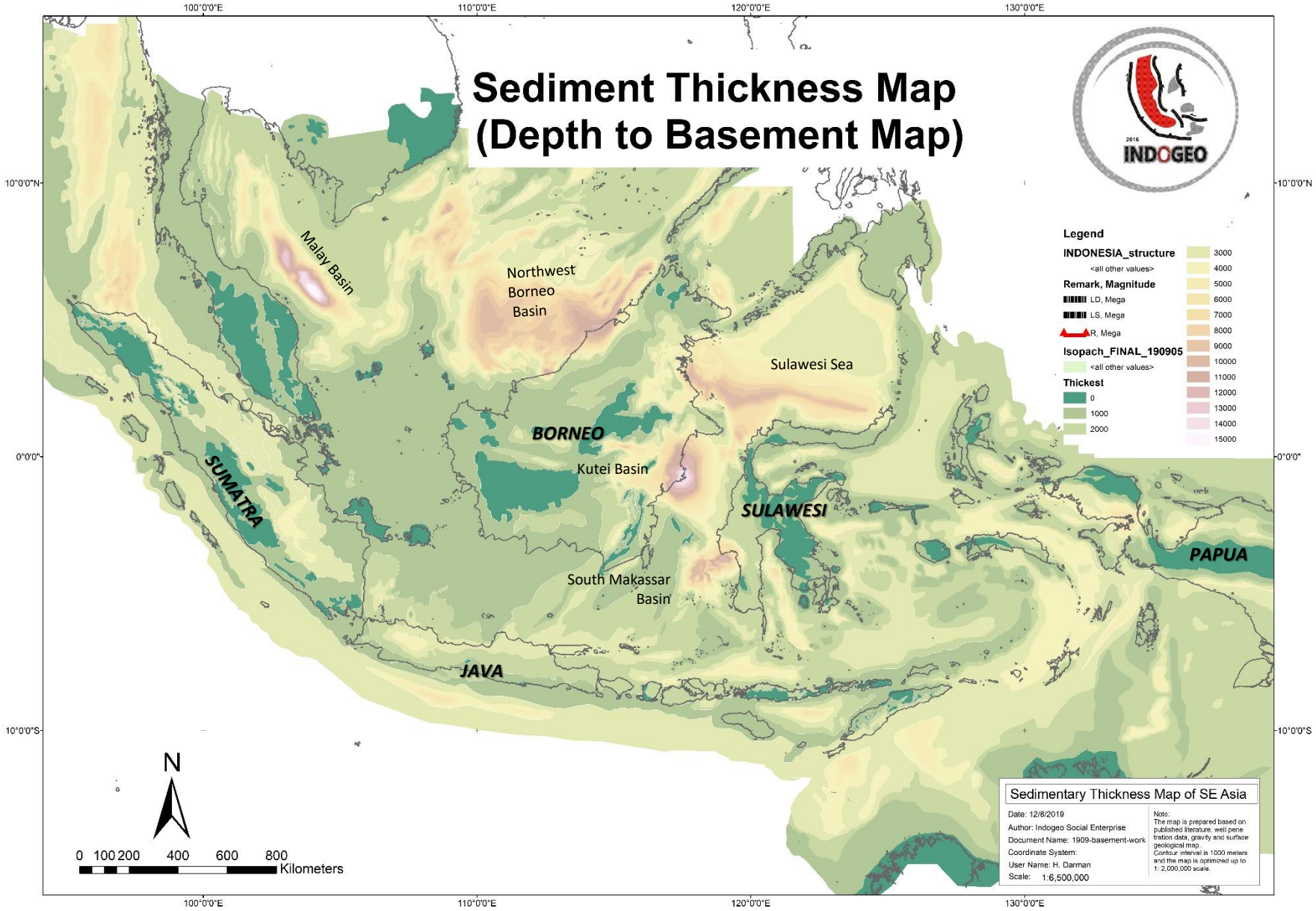


Figure 12: *Sediment thickness map of Indonesian and some SE Asian basins*

The following list shows the benefits of using integrated sediment thickness map, when the map is overlain with other data, such as:

1. Fields, discoveries and wells with shows, also hydrocarbon seeps, which are able to highlight proven petroleum system and indication of richness potential to add reserves in each basin. Integrating them with Estimated Ultimate Recoverable oil and gas data will help to validate yet to find hydrocarbon resources. Outside nearby area will be potential for step-out lower risk exploration.
2. Exploration wells and seismic lines, which will show indication of exploration maturity and highlight lightly explored area with significant remaining resources potential.
3. Basin outlines, geothermal gradient, heat flow and source rock type maps, which can indicate thick sediment with best regional source rock potential.
4. Tectonic, regional structure and basement type maps, which will highlight potential fracture basement play to connect to source rock potential.

Most geoscientists have finally realized that optimizing available published data can conduct quicker basin evaluation, therefore, the method is appropriate to select focus areas for further studies.

CONCLUSION

A newer version of Sediment Thickness Map is available publicly. It is not only a product of stitching existing published map but also using gravity, well data and controlled by basement outcrops. This map is expected to help both geoscientist and non-geoscientists to understand basin outline maps which are generated by previous authors. The sediment thickness map shows thickness variety across the sedimentary basins in Southeast Asia, especially in Indonesia.

REFERENCES

Anderson, B.L., J. Bon and H.E. Wahono, 1993. Reassessment of the Miocene stratigraphy, paleogeography and petroleum geochemistry of the Langsa Block in the offshore North Sumatra Basin. Proc. 22nd Ann. Conv. Indon. Petroleum Assoc. (IPA), Jakarta, 1, p. 169-189.Barber and Crow, 2005.

Pertamina - BEICIP-FRANLAB, 1992. Global Geodynamics, Basin Classification and Exploration Play-types in Indonesia.

BPMIGAS/LAPI-ITB, 2008. Peta Cekungan Sedimen Tersier Indonesia, included as a slide pack in Satyana, A., 2011, Tectonics, Structures, and implications for Petroleum System: Cases from Indonesia, AAPG Student Chapter - UGM

Ginger, D. and K. Fielding, 2005. The petroleum systems and future potential of the South Sumatra basin. Proc. 30th Ann. Conv. Indon. Petroleum Assoc. (IPA), Jakarta, p. 67-89.

Hamilton, W, B., 1974. Tectonics of the Indonesian Region, USGS, Professional Paper 1078.

Hardy, L, R., Muchsin, S., Ichram, L. O., Samuel, L., and Purnomo, E., 1997. Application of the Petroleum System Concept to Reconnaissance Assessments of Mature and Emerging Producing Basins, with Examples from Indonesia, Proceedings of an International Conference on Petroleum Systems of SE Asia and Australasia, Indonesian Petroleum Association.

Heidrick, T.L., Aulia, K., 1993. A structural and Tectonic Model of The Coastal Plain Block, Central Sumatera Basin, Indonesia. Indonesian Petroleum Association, Proceeding 22th Annual Convention, Jakarta, Vol. 1, p. 285-316

Kenyon, C. S. 1977. Distribution and Morphology of Early Miocene Reefs, East Java Sea., Proceeding of the Indonesian Petroleum Association, 6th Annual Convention.

Nawawi, A., S. Anwar, N. Heriyanto, M. Abdullah, B. Mertani, A. Kohar, C.V. Ponto, H. Darman, W. Ardana, C.A. Caughey, A. Bachtiar, and D. Natanegara, 1996. Petroleum Geology of Indonesian Basins: Principles, Methods, and Application: Volume V, Tarakan Basin, Northeast Kalimantan: Pertamina BPPKA

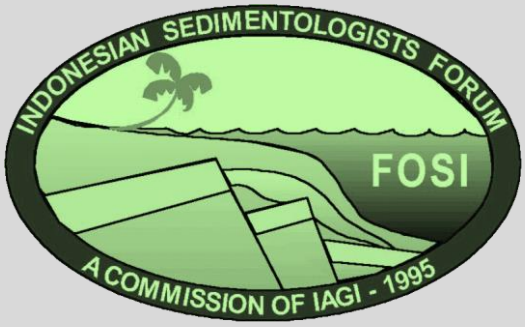
Netherwood, R., 2000. The petroleum geology of Indonesia. Overview of Indonesia ' s oil and gas industry - Geology. Schlumberger Corporation.

Noble, R.A., K.H. Pratomo, K. Nugrahanto, A.M.T. Ibrahim and I. Prasetya, 1997. Petroleum systems of Northwest Java, Indonesia. *In*: J.V.C. Howes & R.A. Noble (eds.) Proc. Conf. Petroleum Systems of SE Asia and Australasia. Indon. Petroleum Assoc. (IPA), Jakarta, p. 585-600

Sujanto, F.X., 1997. Substantial contribution of petroleum systems to increase exploration success in Indonesia. In: J.V.C. Howes & R.A. Noble (eds.) Proc. Int. Conf. Petroleum systems of SE Asia and Australasia, Jakarta 1997, Indon. Petroleum Assoc. (IPA), p. 1-14.

Sumantri, Y.R. & E. Sjahbuddin, 1994. Exploration success in the Eastern part of Indonesia and its challenges in the future. Proc. 23rd Ann. Conv. Indon. Petroleum Assoc. (IPA), Jakarta, 1, p. 1-20.

Sunarjanto, D., Wicaksono, B., Sriwijaya, Munadi, S. and Wiyanto, B., 2008. Updating of Indonesian Tertiary Sedimentary Basin, Proceedings, Indonesian Petroleum Association, 22d Annual Convention & Exhibition.


INDONESIAN SEDIMENTOLOGISTS FORUM
FOSI
A COMMISSION OF IAGI - 1995